Chemical and Biological Technologies in Agriculture

RESEARCH

Open Access

Date pomace polysaccharide: ultrasonic-assisted deep eutectic solvent extraction, physicochemical properties, biological activities, gut microbiota modulation, and rheological properties

Gafar Babatunde Bamigbade[1], Athira Jayasree Subhash[1], Mohammed Tarique[1], Basel al-Ramadi[2], Basim Abu-Jdayil[3], Afaf Kamal-Eldin[1], Laura Nyström[4] and Mutamed Ayyash[1,5*]

Abstract

Background This study utilized ultrasonication-assisted green extraction techniques to explore the physicochemical, rheological, biological, and prebiotic properties, alongside gut modulation abilities of novel polysaccharides extracted from date pomace. The extraction aimed at enhancing the utilization of date pomace, a by-product of date fruit processing, by investigating its potential as a functional food ingredient. The research focused on optimizing the extraction process, understanding the complex structure of the polysaccharides, and assessing their various health-related functionalities.

Results The ultrasonically extracted polysaccharides (UPS) were identified as a mixture of significant bioactive compounds including galacturonic acid, galactose, glucose, arabinose, and fructose, showcasing a high molecular weight of 537.7 kDa. The study found that UPS exhibited outstanding antioxidant activities, with scavenging abilities ranging from 59 to 82% at a concentration of 1000 mg/L. Additionally, UPS demonstrated potent inhibitory effects on α-amylase (83%), α-glucosidase (81%), and ACE-inhibition (45%), alongside strong antiproliferative activities against Caco-2 and MCF-7 cancer cell lines and broad-spectrum antimicrobial properties. Remarkably, UPS also enhanced the abundance of beneficial gut microbiota, including Actinobacteria, Firmicutes, and Proteobacteria, during in vitro fermentations and positively modulated gut metabolic pathways, promoting the production of major short-chain fatty acids. UPS had higher abundance in pathways related to cofactors, vitamins, electron carriers, and prosthetic groups biosynthesis compared to blank.

Conclusions The findings affirm the potential of UPS extracted from date pomace as an innovative and promising functional food ingredient. Its high molecular weight, complex sugar composition, significant antioxidant, antimicrobial, antiproliferative activities, and prebiotic properties make it a valuable resource for promoting health and managing diseases. This study paves the way for further research on the bioavailability and physiological effects of UPS in vivo, highlighting the importance of sustainable utilization of agricultural by-products in developing functional foods that support human health.

Keywords Agro-industrial waste, Functional food, Heteropolysaccharides, Prebiotics, Probiotics

*Correspondence:
Mutamed Ayyash
mutamed.ayyash@uaeu.ac.ae
Full list of author information is available at the end of the article

Graphical Abstract

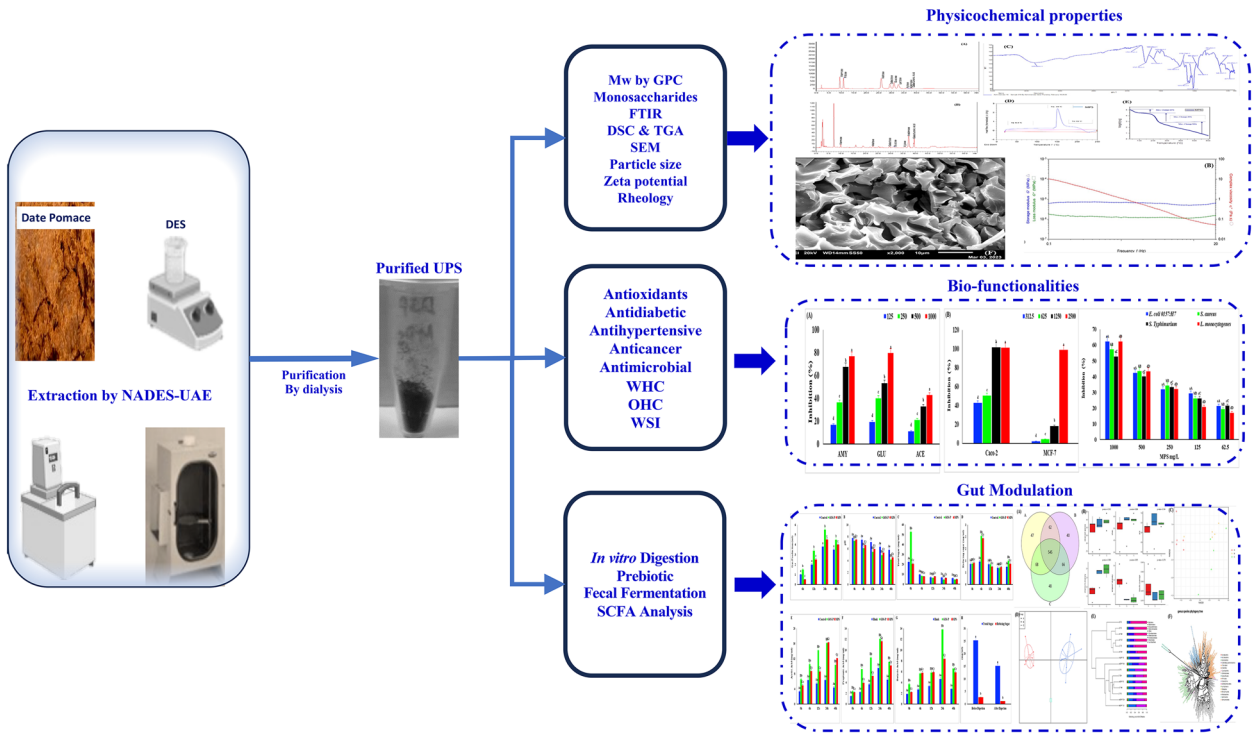

Introduction

Date palm fruits, extensively cultivated and consumed across regions such as Africa, the Middle East, the Gulf Cooperation Council territories, and Central Asia, have experienced a marked increase in utilization owing to their beneficial health properties [1]. This augmented consumption encompasses not only the fruit, but also extends to derivative products including syrups, juices, jams, and pastes, particularly utilizing dates deemed subpar in quality. Dates, being repositories of vital nutrients, are a staple component within the dietary frameworks prevalent in MENA regions [1]. The agricultural and food industries contribute to significant by-product generation; nonetheless, these by-products present opportunities for resource recovery, promoting sustainability and the adoption of circular economies [2]. The processing of date fruits results in various by-products, such as date seeds, pomace, and substandard fruits, all rich in bioactive constituents.

Currently, date pomace (DP) is primarily utilized within animal feed formulations, despite a large proportion being discarded, which leads to environmental detriments. The nutrient matrix of DP, abundant in polysaccharides, proteins, phenolic compounds, and essential vitamins, renders it an opportune candidate for incorporation in animal feeds and as a substrate for the synthesis of high-value products [1]. Scientific investigations have predominantly concentrated on the phenolic content within dates, while the polysaccharides—complex carbohydrates composed of monosaccharide units connected via glycosidic linkages and sourced from various biological origins, including plant, animal, and microbial—have received less focus [3, 4]

Polysaccharides, functioning as dietary fibers, emulsifiers, and stabilizers, are pivotal in food and pharmaceutical industries due to their intrinsic bioactive properties that may confer antitumor, antiglycation, and cardioprotective effects [5, 6]. Their significant role in modulating the gut microbiota, which is essential for digestion, nutrient absorption, and immunomodulation, further highlights the critical interaction between dietary polysaccharides and overall health [7]. Despite their importance, date pomace (DP) polysaccharides remain an underutilized resource within the food industry. Conventional extraction methods for polysaccharides, which typically rely on solvent use and are energy-intensive, are

fraught with inefficiencies, thus bolstering the transition towards more eco-friendly extraction techniques [8].

Emerging as a more sustainable option, deep eutectic solvents (DES), consisting of benign metabolites, are gaining recognition for their superior efficacy in the extraction of polysaccharides by disrupting intermolecular interactions and improving solubility [9]. Acidic DES, like ChCl:CA, are particularly promising due to their cost-effectiveness, recyclability, and ability to enhance bioactivity [10]. The use of ultrasound-assisted extraction (UAE) has been lauded for enhancing extraction efficiency while minimizing energy and solvent consumption, and for its capacity to preserve the integrity of thermally labile compounds. The combined application of DES and UAE represents a forward-thinking approach, outperforming traditional methods in terms of efficiency, cost, and environmental impact [10]. Evidence also suggests that the ultrasonic parameters (cavitation, frequency, intensity, and mass transfer) can alter polysaccharides' structural and chemical characteristics, thereby affecting their physicochemical and biological attributes [11]. Additionally, ultrasonic degradation of *Plantago asiatica* L. seed polysaccharides has been linked to increased prebiotic activities, modulation of gut microbiota, and short-chain fatty acid (SCFA) production [12]. Therefore, investigating the effects of ultrasonication on the polysaccharides of DP may yield notable findings.

To date, the endeavor of extracting polysaccharides from date pomace (UPS) utilizing an ultrasound-assisted deep eutectic solvent method and the subsequent impact on their physicochemical, structural, and biofunctional properties has not been documented. This study aimed to (1) investigate the extraction of UPS using ultrasound-assisted DES and conduct a thorough physicochemical characterization; (2) assess the rheological, functional, and biological properties of UPS, at various concentrations, including its capacity for antioxidant, antidiabetic against α-amylase and α-glucosidase enzymes, ACE-inhibition, antiproliferative activity against Caco-2 and MCF-7 cell lines, and antimicrobial activities against four pathogenic bacteria; (3) evaluate the prebiotic efficacy of UPS by its ability to stimulate growth of six well-known probiotic bacteria and modulate human gut microbiota and SCFA production through in vitro fecal fermentation.

Materials and methods

Materials

Approximately 20 kg of fresh wet date pomace (DP) residue was obtained from Al Foah Date Processing Industry in Al Ain, Abu Dhabi, United Arab Emirates, and stored at −20 °C for further analysis. Choline chloride (ChCl) and citric acid (CA) were procured from Sigma-Aldrich Inc. (St. Louis, Missouri, USA). All other chemicals and reagents employed were of high analytical grade and were sourced from Sigma-Aldrich, unless otherwise indicated.

Preparation of deep eutectic solvent (DES)

The DES was prepared following the heating and stirring method described by Shafie and Gan [13]. ChCl and CA were mixed in a 1:1 molar ratio with 30% water. These conditions were chosen based on preliminary trials with different molar ratios (1:1, 1:2, 1:3, 1:4, 2:1, and 3:1) and various water percentages (20–50%) and 1:1 gave the highest amount of polysaccharides evaluated with phenol–sulphuric acid method. The mixture was continuously stirred with a magnetic bar and heated on a heat stirrer (Stuart UC152, UK) at 80 °C until a homogeneous and transparent eutectic liquid was formed.

Pretreatment of date palm residue with deep eutectic solvent

A slightly modified method based on Yang et al. [14] was employed for defatting. Specifically, a 1:5 (w/v) ratio of DP to hexane was continuously stirred on a magnetic stirrer for 4 h. The DP was separated from hexane by draining it over muslin cloth and air-dried overnight in a fume hood at ambient temperature, then stored at −20 °C for further analysis. During the pretreatment, 0.5 g of DP was added to 10 mL of the DES and incubated at 80 °C for 120 min with constant shaking at 250 rpm in a WSB shaking water bath (Witeg, Germany). The heated mixture was centrifuged at 10,000×*g* at 5 °C for 15 min (Centrifuge 5804, Eppendorf AG, Germany). The supernatant was separated using muslin cloth and analyzed for the total amount of extracted polysaccharides using the phenol–sulfuric acid method described by Cuesta et al. [15].

Optimization of DP pretreatment with deep eutectic solvent

The experimental design for evaluating the efficiency of DES pretreatment was performed using Design-Expert Ver. 8.1.5 (Stat-Ease Inc., Minneapolis, MN, USA). Response Surface Methodology (RSM) was employed for the experimental design, and a total of 26 runs were conducted (see Table S1). The polysaccharide extraction yield was considered the response variable for the design experiments, and a Central Composite Design (CCD) was carried out to determine the optimal pretreatment conditions.

Optimization of ultrasound-assisted deep eutectic extraction of polysaccharides

The polysaccharides from the DES-pretreated DP mixture were extracted using a probe-type ultrasonic system (SFX550, Branson, Mexico) at 80 m amplitudes for 15 min. The sonicated mixture was centrifuged and quantified, as described in Section. "Pretreatment of date palm residue with deep eutectic solvent". A 2^3 experimental design was carried out to evaluate the extraction efficiency of UAE for polysaccharides extraction. The experiment was designed with RSM using Design-Expert Ver. 8.1.5, and a total of 10 runs were obtained (see Table S3). CCD was applied to determine the optimal UAE conditions. The polysaccharide extraction yield was considered the response variable for the design. The mathematical model corresponding to the CCD is presented in Eq. 1.

$$Y = \beta_0 + \beta_1 X_1 + \beta_2 X_2 + \beta_{11} {X_1}^2 + \beta_{22} {X_2}^2 + \beta_{12} X_1 X_2 + \epsilon, \quad (1)$$

where Y represents the response of yield, β_0 is the intercept, β_1 and β_2 are the linear coefficient, β_{11}, β_{22} are quadratic and β_{12} represents the interaction coefficient. The experimental analyses were conducted in triplicates, and the data obtained were analyzed with regression analysis to select the optimal conditions for the UAE extraction of polysaccharides.

Purification of crude polysaccharides

Deproteinization and purification of UPS were conducted according to the method described by Ali et al. [16] with slight modifications. The crude polysaccharides were mixed with four volumes of chilled absolute ethanol and stored at 4 °C for 24 h, followed by centrifugation at 5000 *xg* for 20 min. Afterward, the precipitated polysaccharides were mixed with 16% (w/v) trichloroacetic acid to eliminate the presence of any proteins. The mixture was centrifuged at 15,000×*g* at 4 °C for 20 min. The supernatant was purified using Slide-A-Lyzer™ G2 dialysis cassettes (10 kDa MWCO) (Thermo Fisher Scientific) against deionized water for 72 h at 4 °C. The UV–Vis spectrometer (Epoch™ 2, Bio-Tek, VT, USA) did not detect absorbance at 260 and 280 nm, indicating no presence of proteins or nucleic acids. The purified UPS was freeze-dried and stored at -20 °C for further analysis. The total carbohydrate content was quantified as reported in Sect. "Pretreatment of date palm residue with deep eutectic solvent".

UPS characterization

Molecular weight (Mw) and monosaccharide composition determination

The method reported by Bamigbade et al. [17] was employed to evaluate the Mw using gel permeation chromatography (GPC). Before injection into the SIL-20AC autosampler of the HPLC system (Shimadzu, Kyoto, Japan), the sample underwent filtration through a 0.22-µm syringe filter. The system, which was equipped with a refractive index detector (RID-20A) and a Shimpack GPC-802 column, maintained a constant temperature of 40 °C. Distilled water with a flow rate of 1 mL/min was used to elute the samples. To determine the molecular weight (Mw), calibration curves based on pullulan standards were employed. Monosaccharides composition was determined according to Qiao et al. [18]. Briefly, 2 M trifluoroacetic acid (TFA) (1 mL) was used to hydrolyze the purified UPS (25 mg) at 105 °C for 4 h in a heating block to fractionate the sample into constituent monosaccharides followed by methanol addition (1 mL) and purging with nitrogen until the hydrolysate become dried. The dried hydrolysates was then reconstituted with 1 mL deionized water, then 50 µL of the mixture was added to 50 µL of 0.6 M NaOH, 100 µL of 0.5 M methanolic 1-phenyl-3-methyl-5-pyrazolone (PMP) and vortex. The reaction mixture was completely derivatized by incubating in a water bath for 70 min at 70 °C. After heating, the mixture was cooled and neutralized with 120 µL 0.3 M HCl, vortex and make up to 1 mL with deionized water. The derivatized hydrolysate was extracted three times using an equal amount of chloroform and centrifuged at 10,000×*g* for 10 min to remove the organic phase (chloroform layer). Monosaccharide standards (arabinose, fructose, galactose, galacturonic acid, glucose, lactose, maltose, mannose, ribose, and xylose) were hydrolyzed and derivatized as described for the UPS. The derivatized UPS was filtered using a 0.45-µm membrane filter and injected into the Thermo C18 (250×4.6 mm, 5 µm) column in the Shimadzu HPLC system equipped with an SPD-M20A photodiode array using the following conditions: mobile phase A: 0.1 M ammonium acetate, mobile phase B: acetonitrile; flow rate: 1.5 mL/min; UV detector: 245 nm; injection volume: 20 µL; column temperature: 30 °C. A gradient program with varied mobile phase (A: 0.1 M ammonium acetate, mobile phase B: acetonitrile) concentration at flow rate: 1.5 mL/min and column temperature of 30 °C was used.

Fourier transform infrared (FTIR) spectroscopy

FTIR spectroscopy was performed as per the protocol described by Ali et al. [16]. The UPS powder was applied onto a diamond/ZnSe crystal plate (PerkinElmer Inc., CA, USA). The plate was then scanned 16 times using the Spectrum Two FT-IR Spectrometer (PerkinElmer). The scanning was conducted from 4000 to 400 cm^{-1} at a resolution of ± 4 cm^{-1}, and the temperature was maintained at 23 ± 0.1 °C.

Thermal properties

The thermogram of UPS was determined using a differential scanning calorimeter (DSC 25, TA Instruments, DE, USA) as outlined by Sasikumar et al. [19]. UPS (25 mg) was heated in a sealed aluminum pan from 20 to 250 °C at 10 °C/min under a constant N_2 supply. The TGA analysis was conducted to investigate the weight loss as described by Fatahi and Tabaraki [20] with slight modification. UPS (5 mg) was heated from 25 to 600 °C at 10 °C/min with a constant N_2 supply.

Scanning electron microscopy (SEM)

The surface morphology and microstructure were observed using a JEOL JSM-6010LA scanning electron microscope (SEM, Akishima, Tokyo, Japan) operated at an accelerated voltage of 20 kV. A 5 mg of UPS was coated with a thin gold coat using a Cressington 108 Auto Sputter Coater (Ted Pella Inc., Redding, CA, USA) before analysis [16].

Particle size and zeta potential analysis

The particle size distribution and zeta potential charge were determined according to Ali et al. [16]. UPS was diluted to 1 mg/mL with deionized water and placed in the cells of the NanoPlus-3 Particulate Systems (Micromeritics Instrument Corp., GA, USA).

Physical and rheological properties

Three rheological tests were performed on the crude aqueous solution of UPS (5 mg/mL) using a rheometer (Discovery Hybrid HR-2, TA Instruments, DE, USA) according to Ali et al. [16]. A 50 mm geometry cone plane at a 50 µm gap, 1° cone angle, and 25 ± 0.1 °C plate-controlled temperature was employed for the analyses. Data were analyzed using TRIOS 5.2 software.

Amplitude and frequency sweep tests

The linear viscoelastic region of UPS solution was evaluated using an amplitude sweep test in the strain range of 0.1–10% at a constant frequency of 1.0 Hz. The frequency sweep test was used to estimate the viscoelastic behavior of UPS at a frequency range of 0.1–10 Hz and a strain of 0.8% within the linear viscoelastic region.

Time-dependent behavior

UPS solution was subjected to low and high shearing conditions as described by Rütering et al. [21] to determine structural deterioration and recovery. The storage (G') and loss (G") moduli were measured over three-time segments: (200 s, 0.2 Pa), (60 s, 50 Pa), and (400 s, 0.2 Pa).

Water binding capacity (WBC) and fat binding capacity (FBC)

The WBC and FBC of UPS were determined according to Jia et al. [22]. Briefly, 75 mg of freeze-dried UPS was dissolved in 1.5 mL of deionized-distilled water or sunflower oil in a centrifuge tube of known weight and dispersed with a vortex for 5 min at room temperature. The mixture was centrifuged at 15,000×*g* for 30 min, the supernatant was removed, and the residues were weighed. WBC and FBC were calculated in percentages using Eq. 2.

$$\mathrm{WBC/FBC(\%)} = \left(\frac{\mathrm{Water/oil\ bound\ weight}}{\mathrm{Total\ dry\ sample\ weight}}\right) \times 100. \tag{2}$$

Water solubility index (WSI)

The WSI was evaluated according to Ali et al. [16]. Briefly, 100 mg of UPS was mixed with 2 mL of deionized water in a centrifuge tube with a known weight and vortexed until fully dissolved, followed by centrifugation at 12,000×*g* for 10 min, and the supernatant was freeze-dried overnight. The WSI value was determined with Eq. 3.

$$\mathrm{WSI(\%)} = \left(\frac{\mathrm{Dry\ weight\ after\ lyophilization}}{\mathrm{Total\ sample\ weight}}\right) \times 100. \tag{3}$$

Biofunctional activities of UPS

All the biofunctional activities were carried out according to methods detailed in [23, 24] unless otherwise mentioned.

Antioxidant capacities

Radical scavenging by DPPH and ABTS In this section, the radical scavenging activities of UPS at various concentrations (125, 250, 500, and 1000 mg/L) were assessed using 1, 1-diphenyl-2-picrylhydrazyl (DPPH) and 2,2′-azino-bis(3-ethylbenzene-thiazoline-6-sulphonic acid) radical (ABTS•+). The absorbance was measured at specific wavelengths (517 nm for DPPH and 734 nm for ABTS•+) following established methodologies. The percentage radical scavenging rate of DPPH and ABTS·+was calculated using Eq. 4.

$$\text{Scavenging rate (\%)} = \frac{(\text{Blank absorbance} - \text{UPS absorbance})}{\text{Blank absorbance}} \times 100. \quad (4)$$

Superoxide radical scavenging activities This section investigated the superoxide scavenging activities of purified UPS at different concentrations using superoxide dismutase (SD) and superoxide anion scavenging (SAS) assays. Absorbance measurements were taken at 420 nm for SD and 320 nm for SAS. The inhibition rate of pyrogallol oxidation was calculated using Eq. 4.

Reactive oxygen species (ROS) scavenging activities Here, the inhibition of reactive oxygen species by purified UPS was evaluated using hydrogen peroxide (HP) and hydroxyl radical scavenging (HRS) assays. Absorbance measurements were conducted at 230 nm for HP and 536 nm for HRS. The scavenging activity was calculated using Eq. 4.

Metal chelation For MC activity, 1 mL of UPS was mixed with 2 mL of water, 0.4 mL of ferrozine solution (6 mM), and 80 µL of $FeCl_2$ solution (4 mM) in a glass tube. The mixture was then incubated at room temperature for 20 min. The absorbance was measured at 562 nm, and result was calculated in µg/mL.

FRAP and reducing power The antioxidant power of purified UPS was determined using ferric reducing antioxidant power (FRAP) and reducing power (RP) assays. Absorbance measurements were taken at 593 nm for FRAP and 700 nm for RP. The results were calculated in terms of µg/mL equivalent to ascorbic acid using equations based on standard curves.

Total antioxidant capacity (TAC) The total antioxidant capacity (TAC) of UPS was evaluated through a specific method involving the preparation of a TAC reagent and absorbance measurements at 695 nm. The results were calculated in terms of µg/mL equivalent to ascorbic acid using an equation based on a standard curve.

Inhibition of α-amylase and α-glucosidase activities

The antidiabetic activity of purified UPS was assessed by evaluating its capacity to inhibit α-amylase and α-glucosidase. These assays involved specific reagents, incubation, and absorbance measurements at specific wavelengths. The absorbance was recorded at 400 nm. The percentage rate of inhibition was calculated using Eq. 3.

$$\text{Inhibition (\%)} = \frac{(\text{Blank absorbance} - \text{UPS absorbance})}{\text{Blank absorbance}} \times 100. \quad (5)$$

Angiotensin-converting enzyme (ACE) inhibition

The ACE inhibitory activity of purified UPS was evaluated according to Tarique et al. [23]. Absorbance measurements at 228 nm were used to calculate the percentage rate of inhibition using Eq. 5.

Antiproliferative activity

The antiproliferative effects of purified UPS on Caco-2 and MCF-7 cancer cell lines were assessed using a specific procedure. This involved incubation with the cells, addition of reagents, and absorbance measurements at specific wavelengths. Percentage cytotoxicity was calculated based on the ratio of OD570/OD605 nm:

$$\text{Cytotoxicity(\%)} = \left[1 - \frac{R_{sample} - R_0}{R_{ctrl} - R_0}\right] \times 100 \quad (6)$$

where R_{sample} is the absorbance ratio of OD570/OD605 in the presence of EPS-C70. R_{ctrl} is the absorbance ratio of OD570/OD605 in the absence of UPS [vehicle (positive) control]. R_0 is the averaged background [non-cell (negative) control] absorbance ratio of OD570/OD605.

Minimum inhibitory concentrations (MIC)

The MIC of UPS against four common food pathogens, including *Escherichia coli* 0157:H7 1934, *Salmonella* Typhimurium 02-8423, *Staphylococcus aureus* ATCC 25923, and *Listeria monocytogenes* DSM 20649) was determined through a specific method involving dilution and incubation. Absorbance measurements at 600 nm were used to calculate the percentage rate of inhibition [23].

In vitro digestion of UPS

The digestibility of UPS was evaluated using the INFOGEST2.0 model for adults, as detailed by Brodkorb et al. [25]. Briefly, 30 mg/mL of UPS was sequentially mixed with in vitro oral, gastric, and intestinal fluids. Total sugar (TS) and reducing sugar (CR) using the crude aqueous solution were assessed according to Bamigbade et al. [17].

Prebiotic properties

The prebiotic properties of the purified UPS were assessed using six probiotic strains: *Lactobacillus acidophilus*, *Lactobacillus delbrueckii* subsp. *delbrueckii*, *Lacticaseibacillus rhamnosus*, *Lacticaseibacillus paracasei* subsp. *paracasei*, *Lactobacillus gasseri*, and

Bifidobacterium breve, following the procedure reported by Yılmaz and Şimşek [26]. The growth kinetics of each probiotic strain at 600 nm for 24 h were measured under different carbon sources.

In vitro fecal fermentation, microbial analysis, and short-chain fatty acid (SCFA) analysis

In vitro fecal fermentation of UPS

The in vitro fecal fermentation was carried out according to the method described by Bamigbade et al. [17]. Briefly, fecal slurry was prepared using an equal amount of fecal samples pooled from four healthy individuals (26–45 years) without recent use of antibiotics. The fecal slurry was mixed with a basal medium and various treatments (blank, galacto-oligosaccharides (GOS-P), and UPS) and then incubated at 37 °C in a shaking water bath for 24 h, as described by Bamigbade et al. [17]. Changes in pH, gas production, total sugar, and reducing sugar during fecal fermentation were evaluated at 0, 6, 12, 24, and 48 h.

Microbial analysis during fecal fermentation

The microbial content for each treatment was analyzed every 6 h during fecal fermentation as per Bamigbade et al. [17]. Briefly, Genomic DNA was extracted using the Genomic DNA Kit (Tiangen, Beijing, China). The V3–V4 regions of 16S rRNA were amplified and analyzed at BGI, Hong Kong. Library construction, concentration, and quality assessment were performed using Agencourt AMPure XP beads and Agilent 2100 Bioanalyzer, respectively. Raw data were filtered using iTools Fqtools fqcheck (v.0.25), and the paired-end reads were merged into a single tag sequence using Fast Length Adjustment of SHort reads (FLASH, v1.2.11). The sequences were clustered into operational taxonomic units (OTUs) with a 97% similarity threshold by UPARSE, while chimeras were removed using UCHIME (v4.2.40). OTU representative sequences were mapped to the tags using USEARCH (v7.0.1090) and aligned against the database for taxonomic annotation using the RDP classifier (v2.2) at a 60% sequence identity. Alpha diversity was calculated using mothur (v.1.31.2), beta diversity was obtained using QIIME (v1.80) and R (v3.1.1), differential species analysis was carried out using linear discriminant analysis effect size (LEfSe), microbial functional annotation was predicted by PICRUSt2 v2.3.0-b, and R (v3.4.10), while correlation analysis and model prediction were performed using R (v3.4.1) and Cytoscape.

SCFA production

The quantification of short-chain fatty acids (SCFAs) produced by UPS after fecal fermentation was evaluated according to Dobrowolska-Iwanek et al. [27] with slight modifications. After 48 h of fermentation, the broth was centrifuged at 15,000×*g* for 20 min, and the supernatant was filtered using 0.45-µm filters. The Shimadzu HPLC system equipped with the SPD-M20A photodiode array detector (PDA) was used for analysis. A Shodex C18M 4E (250 × 4.6 mm, 5 µm) column (Resonac Inc, Japan) was employed with an isocratic mobile phase containing 10 mM monopotassium phosphate, pH 2.4 with phosphoric acid, and 100% acetonitrile (80:20) at a flow rate of 1.5 mL/min and a column temperature of 30 °C. The injection volume was 20 µL with a 7-min run time and a 210 nm UV detector. Standard curves were prepared for acetic, propionic, and butyric acid under the same conditions at different concentrations.

Statistical analysis

The different biological activities conducted in this study were evaluated in triplicates, and the results were expressed as means ± standard deviation. One-way ANOVA was employed to estimate the significance effect of the UPS concentrations using JMP® Student v17 (JMP Statistical Discovery LLC), and Tukey's test was conducted to perform means comparisons ($p < 0.05$).

Results

Optimization and purification of UPS

To optimize DES pretreatment and ultrasonic-assisted extraction (UAE) factors, we employed a CCD. Results are presented in Tables S1 (DES) and S3 (UAE). Experimental data underwent multiple regression analysis using the CCD matrix. Significance of factors' effects and model validation were assessed through analysis of variance (ANOVA), as in Tables S2 (DES) and S4 (UAE). 3D response surface plots are shown in Fig. S1A–H. The highest UPS yield was achieved under these pretreatment conditions: pH 8, 100 °C, solid–liquid ratio 1:10, and 150 min. UAE parameters were set at an amplitude of 80 m and 20 min. Following extraction, UPS underwent deproteinization and purification before lyophilization. The yield of purified UPS was 5060 ± 0.64 µg/mL, determined using a standard glucose curve ($y = 0.0009x + 0.0021$, $R2 = 0.994$).

Characterization of UPS

Characterized UPS had an average molecular weight (Mw) of 537.7 kDa. Chromatogram analysis (Fig. 1A) revealed UPS as a heteropolysaccharide with varying concentrations of galacturonic acid, galactose, glucose, arabinose, and fructose (molar ratio 0.1:0.9:1.0:0.4:0.3).

FT-IR spectra (Fig. 1C) group displayed typical polysaccharide functional. Peaks at 830.7 cm^{-1} and 844.19 cm^{-1} indicated α- and β-conformation pyranose rings, while 952.37 cm^{-1} signals indicated

glycosidic bonds [28]. Absorbance at 1016.71 cm^{-1} and 1171.87 cm^{-1} suggested pyranose ring stretching and C–O–C vibration. Vibrations of C–O–H and C–O–C (polysaccharide fingerprint) were observed from 972.66 cm^{-1} to 1097.91 cm^{-1}, with C–H bending vibration at 1219.06 cm^{-1} [16]. A prominent peak at 1502.97 cm^{-1} indicated C=O stretching of the carboxylic group, and at 1729.54 cm^{-1}, a non-polar C–C bond was observed [29]. Weak absorbance at 1801.3 cm^{-1} and a wide peak at 3369.63 cm^{-1} indicated mannose presence and stretching of O–H in cellulose and water fraction of polysaccharides, respectively [30]. DSC thermogram (Fig. 1D) revealed T_g (50 °C), T_m (100 °C), and T_d (200 °C). TGA showed three-level mass loss: 12.5% (0–100 °C), 37.5% (100–250 °C), and 37.5% (250–550 °C) with 12.5% residual mass (Fig. 1E). Structural morphology from SEM (Fig. 2) revealed a smooth, compact structure with a mixture of large and small particles. Particle size analysis indicated 5829.8 nm (Fig. S2A), and zeta potential was -256.47 mV (Fig. S2B).

Rheological properties of UPS

Viscoelastic characteristics were assessed with dynamic storage (G') and loss (G") moduli in amplitude and frequency sweep tests. In the amplitude test (Fig. 3A), aqueous UPS products were analyzed. Frequency sweep (Fig. 3B) at a constant shear rate of 0.8% and 0.1–10 Hz showed increasing G' and G" with higher frequency, with G' predominating. UPS's structural changes were evaluated in a time-dependent test over three shear periods (Fig. 3C). At a 0.8% shear rate, UPS displayed elasticity (G'> G"). Acceleration to 50% shear made UPS viscous (G' < G"), returning to elasticity at 0.8% shear.

Bioactive properties of UPS

Antioxidant assays

Antioxidant assays (250–1000 mg/L of UPS) showed dose-dependent activities (Table 1). UPS scavenged DPPH and ABTS radicals (17.1 ± 0.72% to 62.9 ± 2.37% and 31.7 ± 0.68% to 82.1 ± 0.81%, respectively). SD and SAS activities ranged from 14.8 ± 1.69% to 61.6 ± 1.95% and 19.4 ± 1.88% to 58.5 ± 1.07%, respectively. HP scavenging increased from 30.0 ± 0.13% at 250 mg/L to 58.5 ± 0.05% at 1000 mg/L. HRS increased from 17.1 ± 0.07% to 81.1 ± 0.53%. MC rate increased from 19.6 ± 0.07% at 250 mg/mL to 62.8 ± 0.59% at 1000 mg/L. Antioxidant power ranged from 461.4 ± 1.83 to 411.4 ± 1.08, 588.6 ± 20.57 to 961.5 ± 5.95, and 13.1 ± 0.18 to 217.0 ± 0.13 µg/mL for FRAP, TAC, and RP, respectively, at 250–1000 mg/L.

Enzyme inhibitory activity assays

The hypoglycaemic activities of UPS were evaluated with α-amylase and α-glucosidase. A

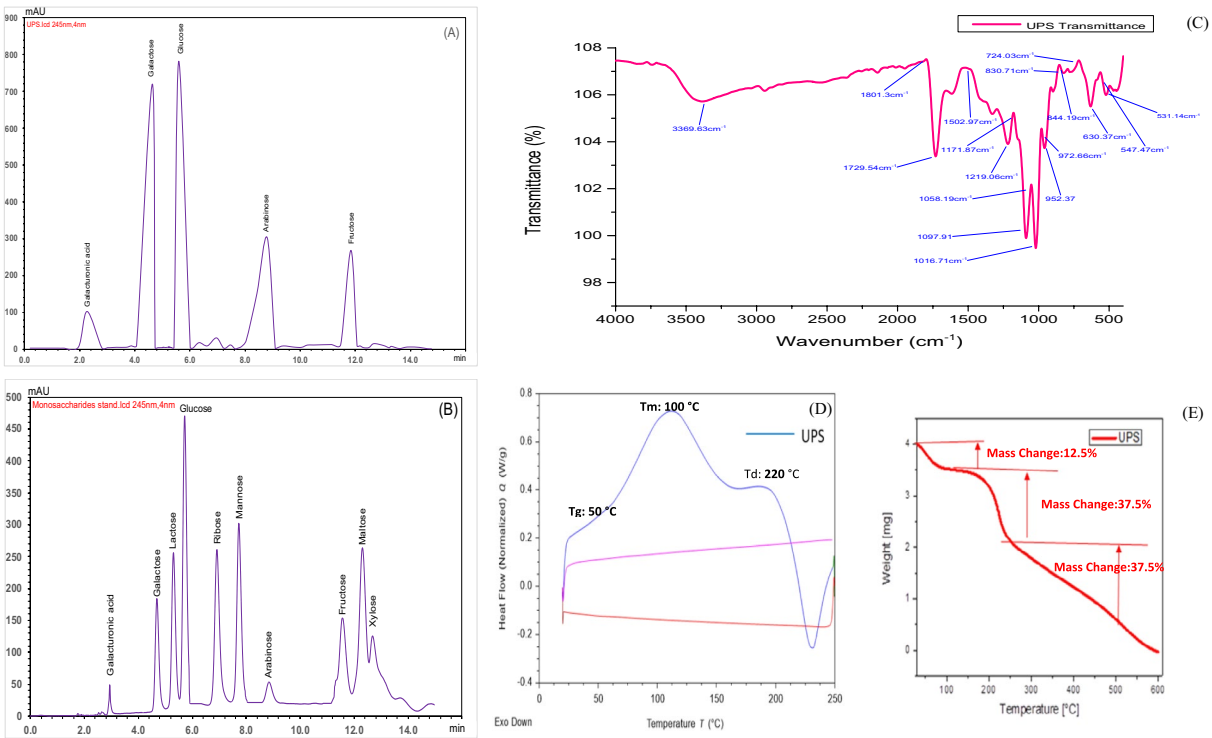

Fig. 1 Monosaccharide composition of UPS (**A**), monosaccharide standards (**B**), FTIR spectrum (**C**), DSC thermogram (**D**), and TGA curve (**E**) of UPS

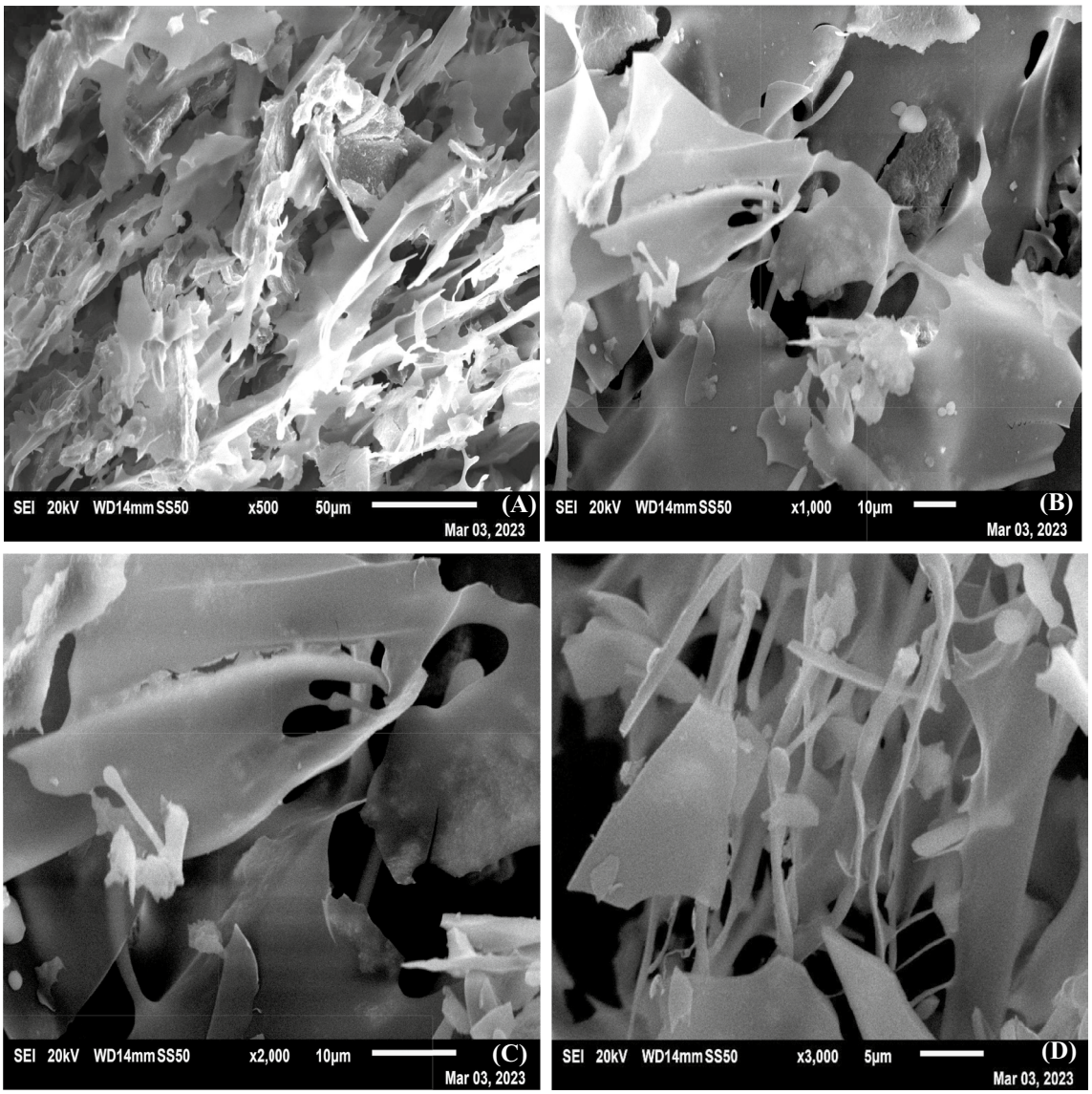

Fig. 2 SEM micrographs of UPS (**A**–**D**) at magnifications 1000X (**A**), 2000X (**B**), and 3000X (**C**–**D**)

concentration-dependent activity was observed, with 83.6 ± 0.48% (IC_{50} = 213.661 µg/mL) for α-amylase and 81.6 ± 0.35% (IC_{50} = 250.316 µg/mL) at 1000 mg/L of UPS, as depicted in Fig. 4A. Additionally, UPS exhibited the highest inhibitory activity of 45.5 ± 0.54% (IC50 = 332.945 µg/mL) at 1000 mg/mL against ACE (Fig. 4A).

Antiproliferative activity

The cytotoxicity of UPS against human carcinoma cells was assessed at four different concentration levels, as illustrated in Fig. 4B. Both Caco-2 and MCF-7 cancer cell lines were employed in this study, and the results indicated a concentration-dependent response. The maximum percentage inhibition was achieved at 2500 mg/L of UPS, with 96.3 ± 0.46% for Caco-2 and 96.6 ± 0.39% for MCF-7, respectively. Notably, MCF-7 cells (IC_{50} = 724.302 mg/L) exhibited greater sensitivity to UPS compared to Caco-2 (IC_{50} = 774.209 mg/L).

Antimicrobial activities

UPS was evaluated for antimicrobial efficacy against four foodborne pathogens at five concentrations (Fig. 4C). Minimum inhibitory concentration (MIC) is defined as

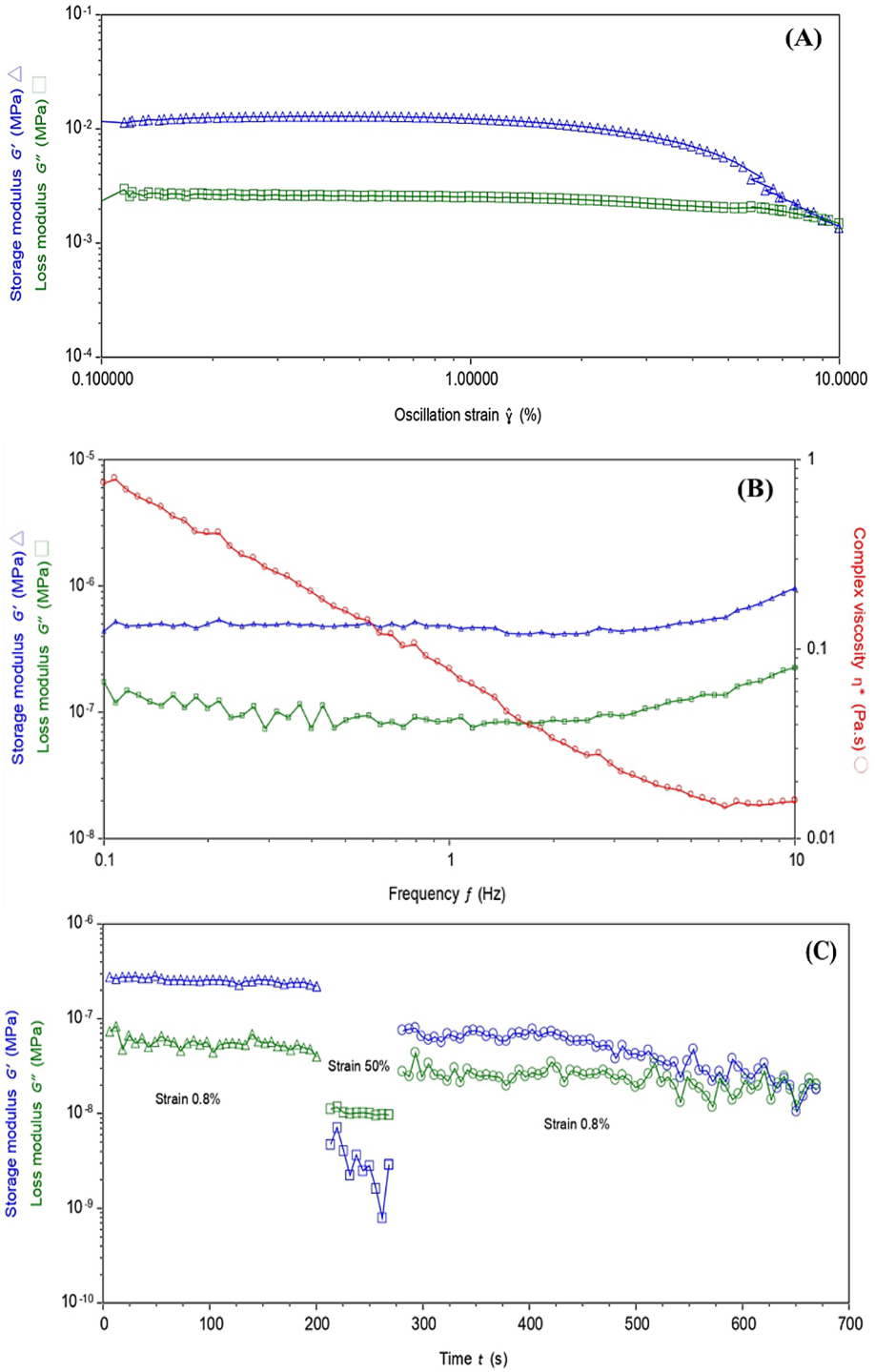

Fig. 3 Rheological properties: **A** amplitude sweep test, **B** frequency sweep test and **C** time-dependent behavior of UPS

a concentration at which 50% of the bacterial population reduces after 24 h. All tested pathogens showed concentration-dependent sensitivity to UPS, with 68.6%, 63.9%, 66.1%, and 65.9% inhibition for *E. coli* 0157:H7, *S. aureus*, *S.* Typhimurium, and *L. monocytogenes*, respectively, at 1000 mg/L.

Table 1 In vitro antioxidant activities of UPS produced by DES-UAE from date pomace at different concentrations

UPS (µg/mL)	DPPH (%)	ABTS (%)	SD (%)	SAS (%)	HP (%)	HRS (%)	MC (%)	LP (%)	FRAP (µg/mL)	TAC (µg/mL)	RP (µg/mL)
125	17.1 ± 0.7^{d}	31.7 ± 0.6^{d}	14.8 ± 1.7^{d}	19.4 ± 1.8^{d}	30.0 ± 0.1^{d}	17.1 ± 0.1^{d}	19.6 ± 0.1^{d}	14.6 ± 0.2^{d}	46.1 ± 1.8^{d}	588.6 ± 20.6^{d}	13.1 ± 0.2^{d}
250	26.9 ± 2.8^{c}	48.9 ± 1.2^{c}	39.2 ± 1.1^{c}	40.4 ± 0.4^{c}	51.6 ± 0.4^{c}	37.4 ± 2.6^{c}	36.9 ± 0.1^{c}	32.1 ± 1.2^{c}	73.9 ± 2.6^{c}	640.7 ± 9.4^{c}	25.5 ± 0.5^{c}
500	45.9 ± 3.7^{b}	65.4 ± 2.7^{b}	52.7 ± 1.7^{b}	48.0 ± 0.1^{b}	58.5 ± 0.1^{b}	57.2 ± 1.5^{b}	50.8 ± 2.2^{b}	53.7 ± 0.2^{b}	269.3 ± 1.8^{b}	796.6 ± 7.2^{b}	113.2 ± 7.5^{b}
1000	62.9 ± 2.4^{a}	82.1 ± 0.8^{a}	61.6 ± 1.9^{a}	59.5 ± 1.0^{a}	58.5 ± 0.1^{a}	81.1 ± 0.5^{a}	62.8 ± 0.6^{a}	80.2 ± 0.5^{a}	411.4 ± 1.1^{a}	961.5 ± 5.9^{a}	217.0 ± 13.0^{a}
IC_{50} (µg/mL)	457.11	295.1	479.94	519.91	361.87	509.53	492.49	510.22	457.9	516.4	527.6

$^{(a–d)}$ Means ± standard deviation with different superscripts at the same column are significantly different ($p < 0.05$)

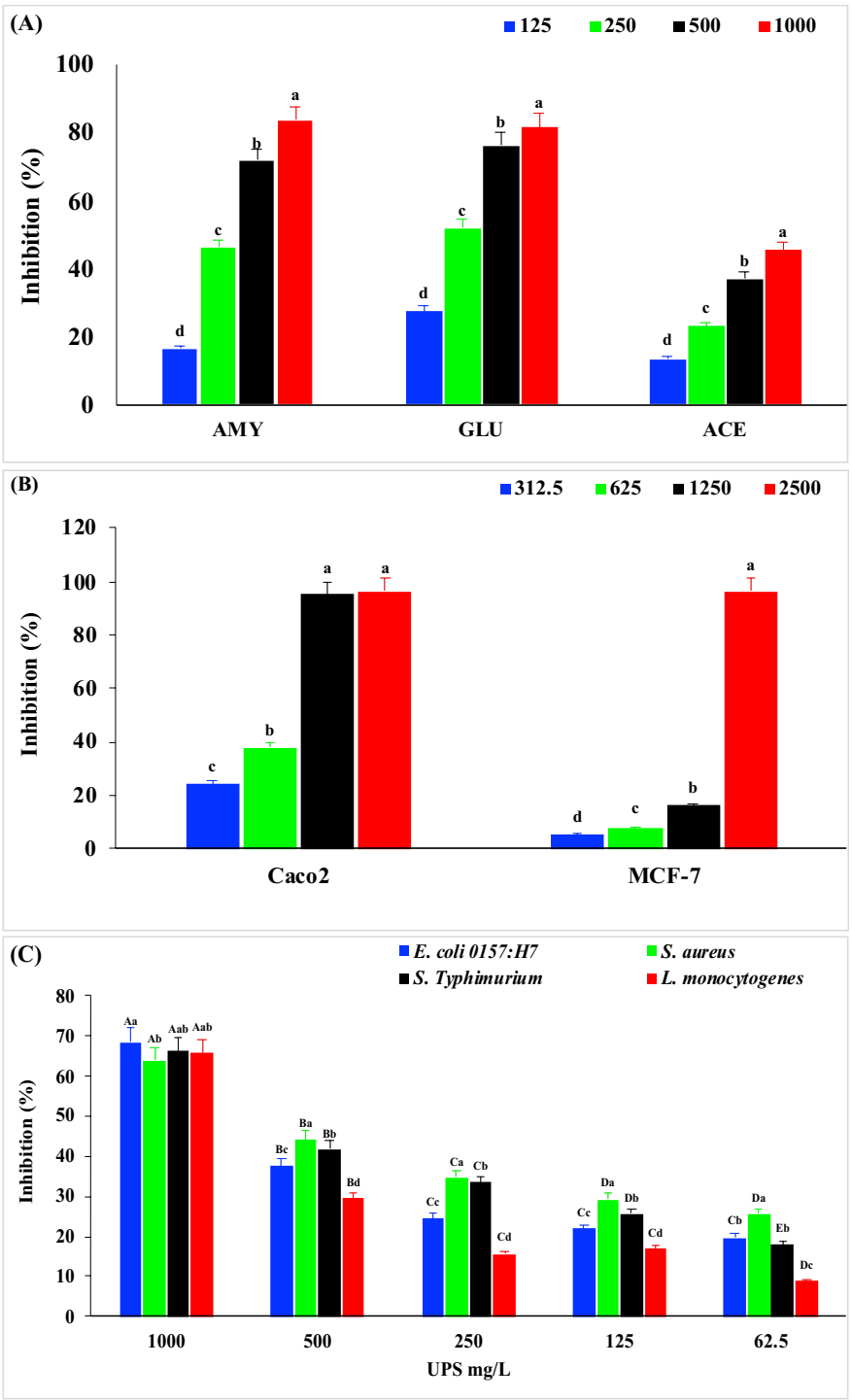

Fig. 4 In vitro bioactivities of UPS at different concentrations (mg/L) (**A**), antiproliferative activities against Caco-2 and MCF-7 cell lines (**B**), and minimum inhibitory concentration (**C**) of UPS. Bars are means ± standard deviations (error bars). $^{a\text{-}c}$ Means with different lowercase letters at the same parameter or concentration differed significantly ($p < 0.05$). $^{A\text{–}E}$ Means with different uppercase letters at the same pathogen strain differed significantly ($p < 0.05$). AMY: α-amylase, GLU: α-glucosidase, and ACE: angiotensin-converting enzyme inhibition

Functional properties of UPS

To estimate the water and oil absorption capabilities of UPS, important functional properties were evaluated, including WBC, FBC, and WSI. The results for these properties were as follows: WBC, 756.2 ± 13.4%; FBC, 941.8 ± 0.7%; and WSI, 39.8 ± 0.9%.

Effect of in vitro digestion on total sugar and CR of UPS

The total sugar content of UPS decreased from 24.2 ± 0.30 to 15.3 ± 0.29, representing a 37% reduction (Fig. S3). Additionally, the C_R decreased from 2.5 ± 0.21 to 0.9 ± 0.91, equivalent to a 63.2% reduction.

Growth stimulation of potential probiotics

To evaluate the prebiotic effects of UPS on six probiotic strains, bacterial growth kinetics were studied over a 24-h period. The study involved the utilization of different carbon sources. The growth of the probiotics in the presence of UPS demonstrated varying degrees of growth kinetics. The cell density ranged between 0.1 nm (control) and 0.7 nm (glucose). With UPS, all six probiotic cultures exhibited reduced lag and exponential phases, and they reached their maximum growth at different times, which fell between the values for GOS-P and glucose. Among the probiotics tested, *Lacticaseibacillus paracasei* subsp. *paracasei* achieved the highest cell density (0.5 nm), while *Lactobacillus gasseri* had the lowest (0.3 nm).

Effect of UPS on in vitro human fecal fermentation

Gas production and pH changes

Gas production increased with fermentation time (Fig. 5A). Maximum gas production of UPS (5 mL) was comparable to GOS-P (5.5 mL), both higher than the control (3.5 mL). Similarly, pH decreased with fermentation time (Fig. 5B). UPS pH reduction from 7.4 to 4.6 was comparable to GOS-P, changing from 7.3 to 4.2. Total and reducing sugars: total sugar content inversely proportional to fermentation time (Fig. 5C). After 48 h, the highest total sugar content in the fermentation broth observed in the control (6.01 mg/mL), while GOS-P and UPS had 4.2 and 4.6 mg/mL, respectively. In contrast, reducing sugar content trend (Fig. 5D) showed initial increase and subsequent decrease, highest values at 6 h for all groups before decreasing further up to 48 h.

Production of short-chain fatty acids (SCFAs)

Concentrations of acetic, propionic, and butyric acids in UPS fecal fermentation products are shown in Fig. 5E–G. All experimental groups exhibited a similar trend, a significant increase in SCFA concentrations with time, up to 24 h, followed by a decline. Highest acetic acid (19.3 mg/mL) produced by UPS, while GOS-P generated highest propionic (12.1 mg/mL) and butyric (13.3 mg/mL) acids. Control group had lowest levels of all quantified SCFAs.

Gut microbiota modulation

Bioinformatic analysis of gut bacteria

After 48 h of fermentation, a total of 883 OTUs identified across all groups, with 541 OTUs shared among all groups. Blank, GOS-P, and UPS groups had 722, 713, and 721 total OTUs, with 61, 55, and 35 unique to each group, respectively. Paired OTUs sharing revealed 66, 54, and 71 OTUs for blank-GOS-P, blank-UPS, and GOS-P-UPS, respectively. Analysis of similarities of the OTUs data indicated significant difference among the OTUs from the three groups. Multiple response permutation procedure confirmed significant differences ($p < 0.05$) among the groups.

Six alpha diversity indexes were used in the study, and their results are presented with refraction curves and boxplots (Fig. 6B). While some diversity measures showed significant differences among the groups, others did not. In the beta diversity analysis, non-metric multidimensional scaling (NMDS) and principal coordinate analysis (PCoA) revealed differences in microbial diversity and species complexities between the groups, with UPS and GOS-P diverging from the control at 48 h. The PCoA enterotype diagram supported these findings, indicating different microbial community compositions in the blank, GOS-P, and UPS groups.

Microbial composition and abundance during fermentation evaluated through OTU taxonomic analysis using RDP classifier Bayesian algorithm. Fig. S6B and S6C depict relative microbial abundance at phylum and genus levels. Major phyla included Firmicutes, Proteobacteria, and Actinobacteria, varying in abundance among the groups. Proteobacteria most abundant in UPS, while Actinobacteria and Firmicutes prominent in GOS-P and blank, respectively. Figure 6E displays relative abundance at order taxon level. Common orders found in all groups included Lactobacilales, Enterobacteriales, Clostridiales, and Bifidobacteriales, highest abundance of Clostridiales and Bifidobacteriales in UPS and Lactobacilales in blank. Several major genera abundant in all groups, including Enterococcus, Escherichia, Bifidobacterium, Blautia, Klebsiella, Streptococcus, and Rombustia. Relative abundances of top 50 genera statistically compared with heatmap (Fig S6D). The abundance of genera in UPS and GOS-P are closely associated and different from blank. Species phylogenetic analysis (Fig. 6F) corroborates results of relative abundances at phylum, order, and genus levels mentioned above.

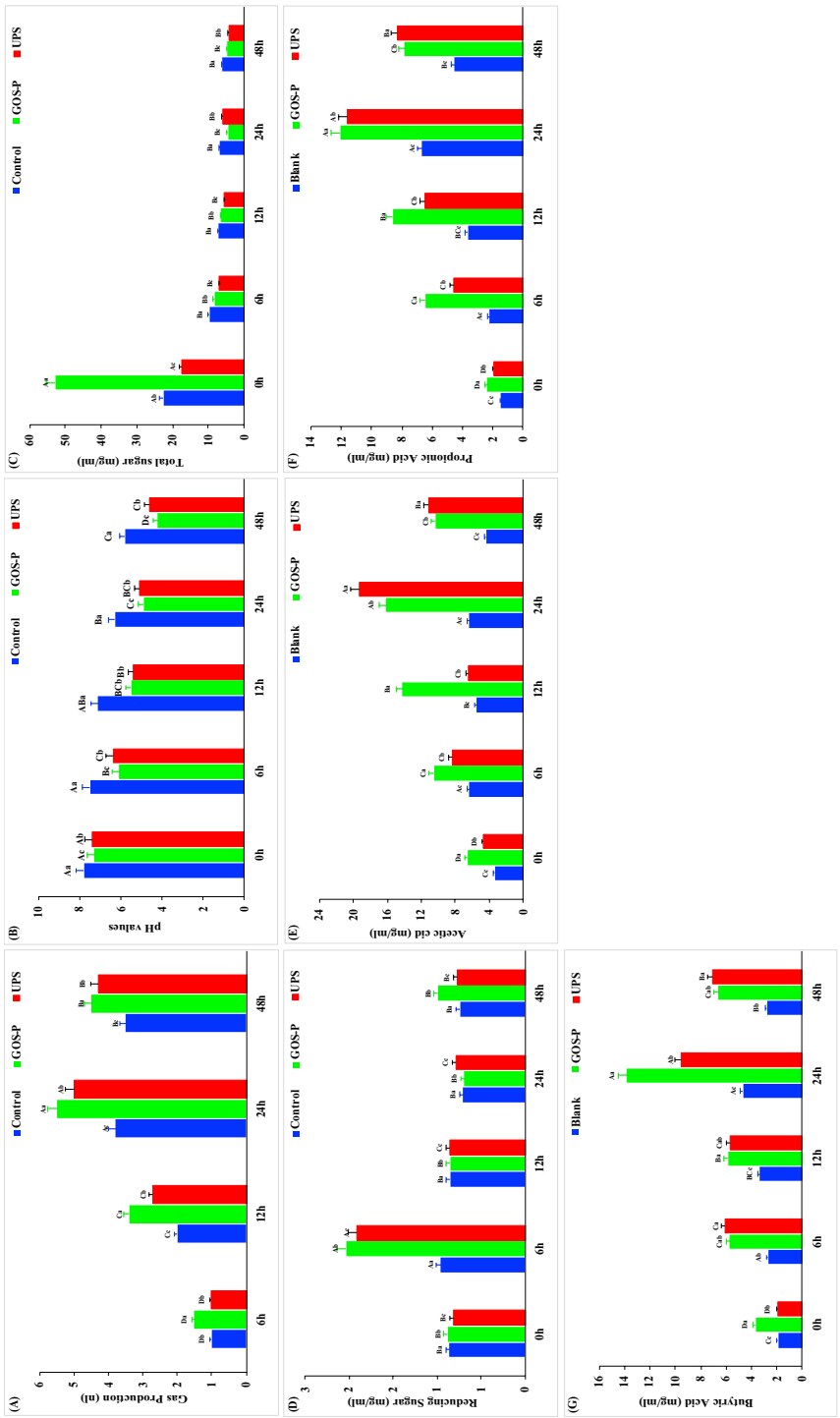

Fig. 5 Gas production (**A**), pH values (**B**), total sugar content (**C**), reducing sugar (**D**), acetic acid content (**E**), propionic acid content (**F**), and butyric acid content (**G**) of during in vitro fecal fermentation: blank (negative control), GOS-P (positive control), and UPS. Bars are means ± standard deviations (error bars). $^{a-c}$ Means with different lowercase letters at same time differed significantly ($p < 0.05$). $^{A-D}$ Means with different uppercase letters, between times, differed significantly ($p < 0.05$)

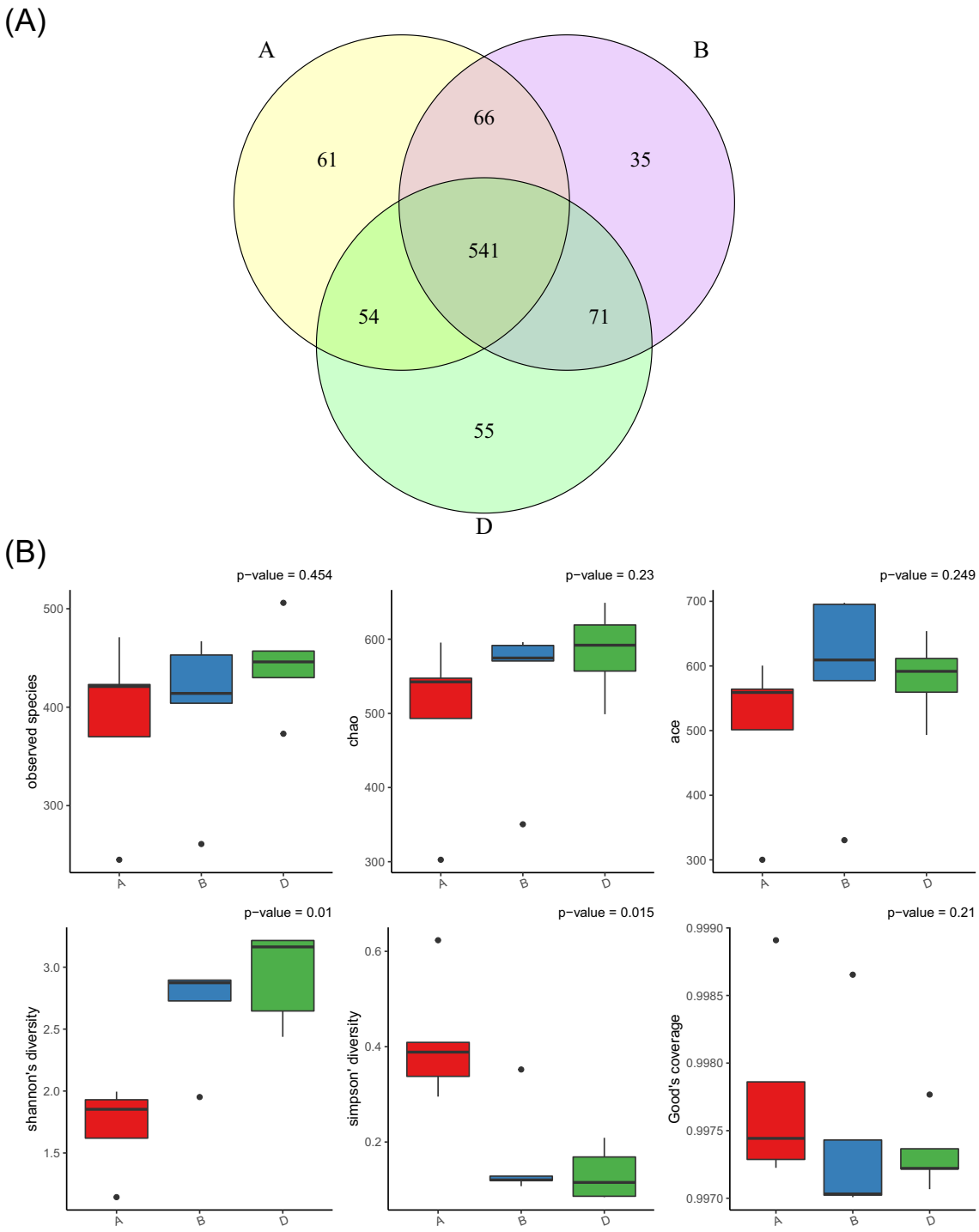

Fig. 6 Effect of UPS on gut microbiome composition during fecal fermentation. Venn diagram (**A**), box plot of different indices of alpha diversity (**B**), NMDS plot (**C**), PCoA plot (**D**), combination graph of UPGMA Cluster Tree and order abundance bar plot (**E**), and species phylogenetic analysis (**F**) of the sample groups. where **A**, **B**, and **D** represent the sample groups blank (negative control), GOS-P (positive control), and UPS, respectively

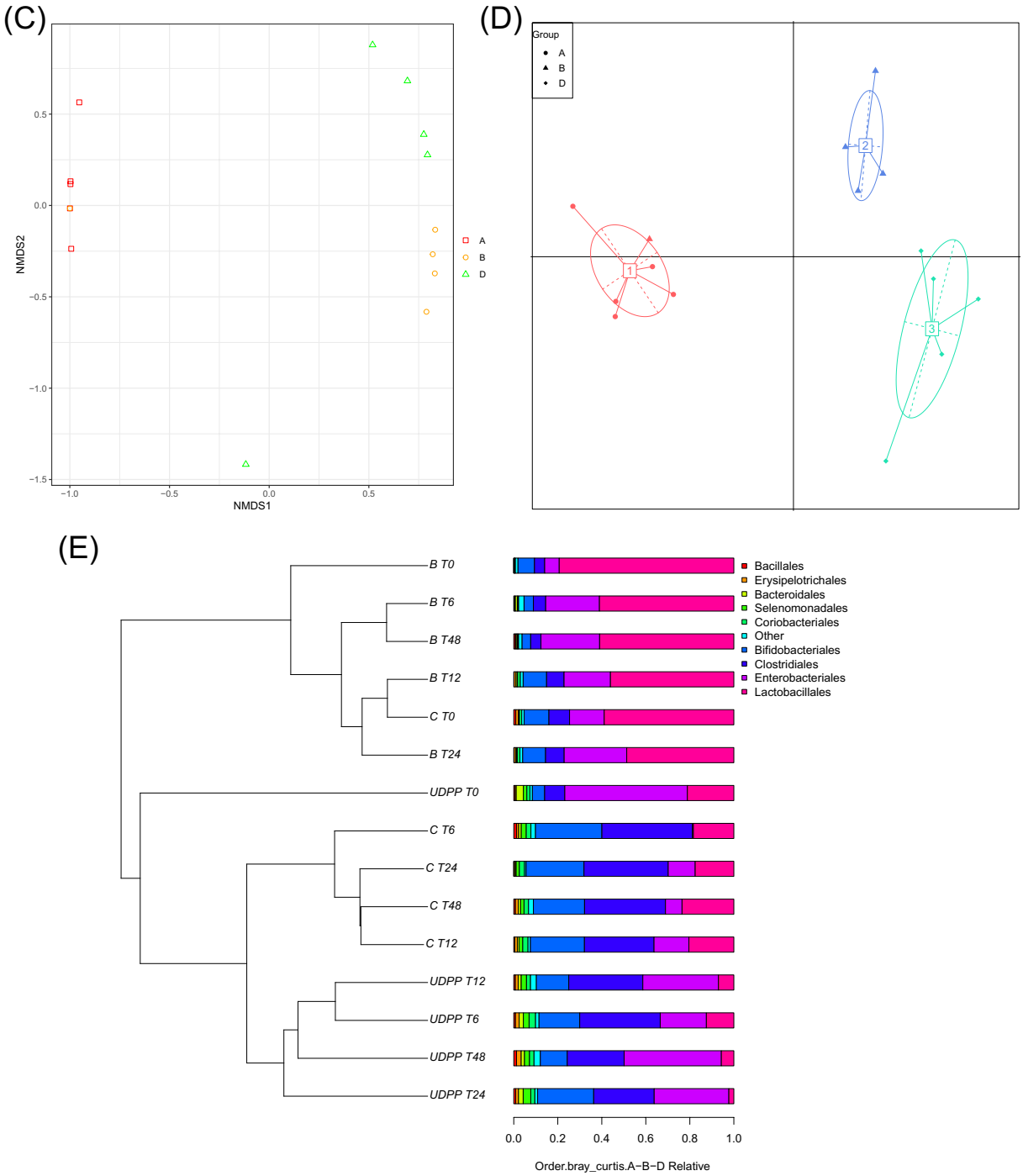

Fig. 6 continued

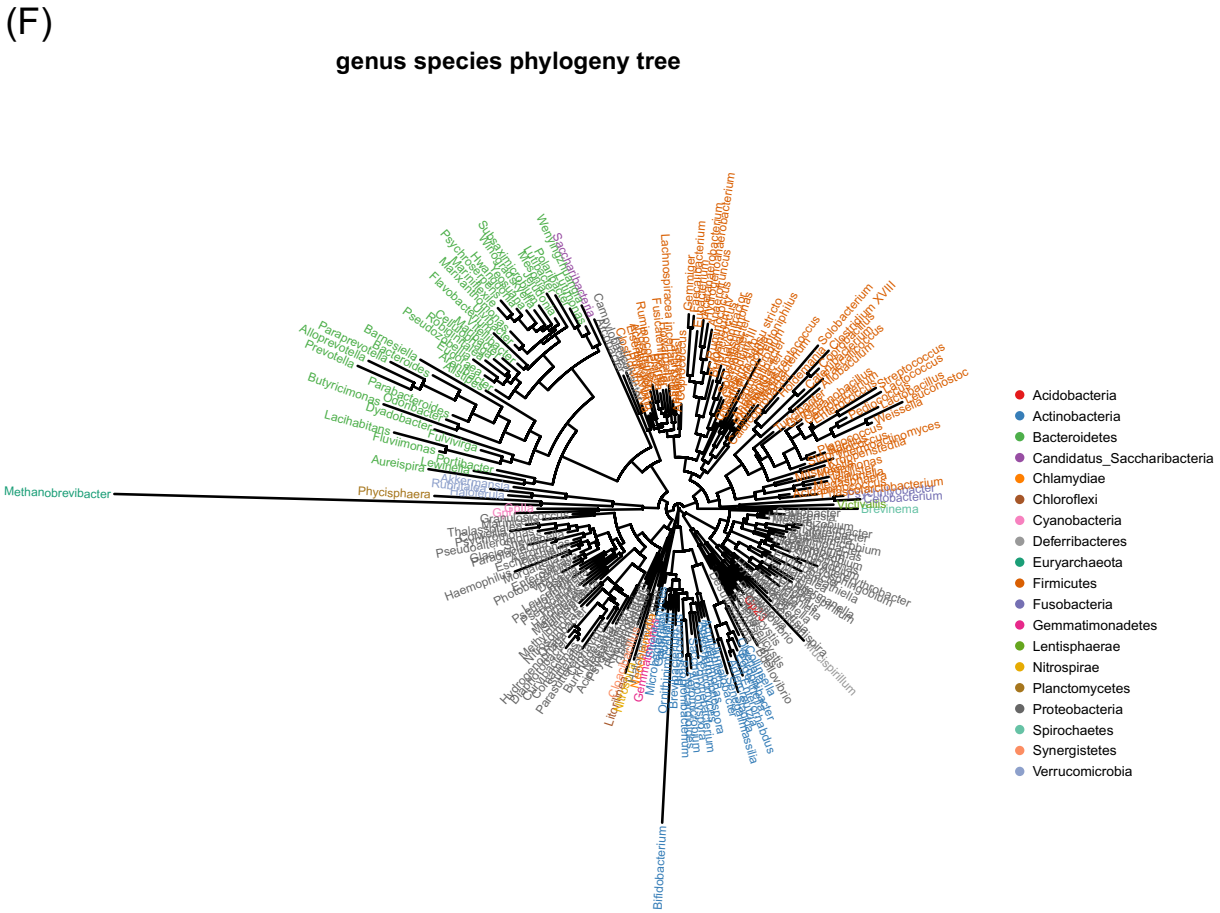

Fig. 6 continued

Overall changes in microbial metabolic pathways

The abundance of microbial metabolic pathways and products during fermentation was evaluated using PICRUSt. The analysis focused on KEGG, COG of proteins, and MetaCyc metabolic pathways. Figure 7A–C presents a relative abundance of metabolic pathways at three different levels. In level 1, all groups had metabolism as highest relative abundance (~ 80%). In level 2, metabolic pathways related to carbohydrates, terpenoids, polyketides, energy, lipids, amino acids, cofactors, vitamins, xenobiotics, and other amino acids are relatively abundant for all groups. In level 3, specific pathways related to glucogenesis, peptidoglycan synthesis, C5-branched dibasic acid metabolism, amino and nucleotide sugar metabolism, biosynthesis of aminoacyl tRNA, lysine and vancomycin antibiotics, thiamine, biotin, tyrosine, and alanine metabolism highly abundant across all groups. COG heatmap (Fig. 7D) revealed that UPS had higher abundance in cell cycle control and division, chromosome partitioning, inorganic ion and coenzyme transport and metabolism, energy production, and conversion compared to blank and GOS-P.

Results of MetaCyc heatmap (Fig. 7E) aligned with KEGG and COG findings. It highlighted enzyme-catalyzed reactions and metabolic pathways of gut microbiota. Results indicated high abundance of pathways related to amino acids, nucleotides, cell structure, fatty acid and lipid biosynthesis, fermentation, and carbohydrate degradation and biosynthesis among the groups. UPS and GOS-P also showed higher abundance in pathways related to cofactors, vitamins, electron carriers, and prosthetic groups biosynthesis compared to blank.

Correlation analysis

The indigenous associations between the fecal microflora were established with Spearman's rank correlation analysis. At $p < 0.05$, the Spearman rank showed a pairwise correlation among the species with positive and negative correlations ranging from strong to moderate and weak. Overall, 14 out of the 15 organisms were

Fig. 7 Effect of UPS on different microbial functions during fecal fermentation. Histograms of KEGG pathways abundance at levels 1–3 (**A**-**C**), heatmap of COG pathways (**D**), heatmap of MetaCyc pathways (**E**), and species spearman coefficients analysis of OTUs in each sample group (**F**), where **A**, **B** and **D** represent sample groups blank (negative control), GOS-P (positive control), and UPS, respectively

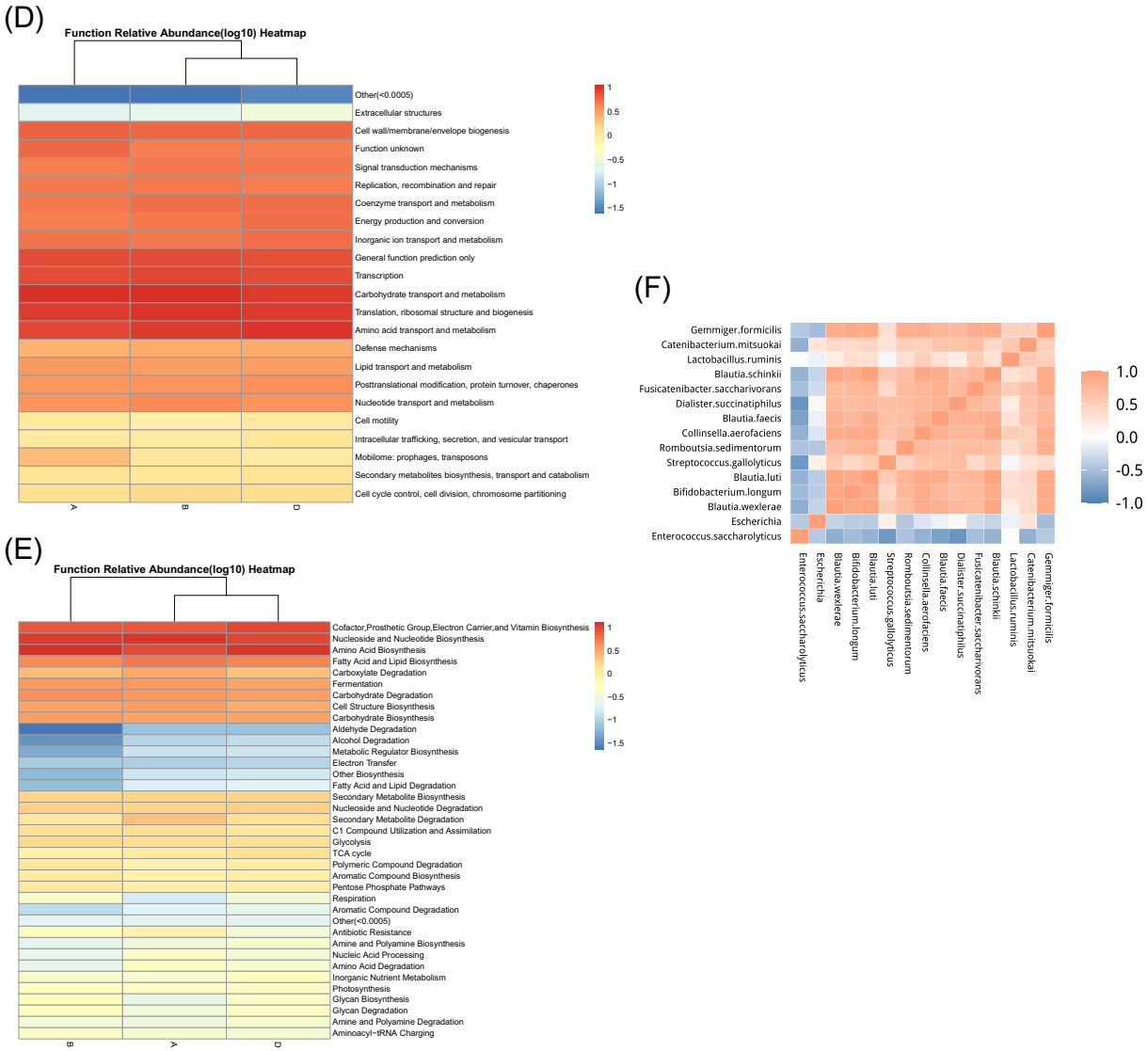

Fig. 7 continued

negatively correlated with *Enterococcus saccharolyticus*, with *Catenibacterium mitsuokai*, *Dialister succinatiphilus*, and *Streptococcus gallolyticus* showing strong negative correlations. Comparatively, only *Catenibacterium mitsuokai, Dialister succinatiphilus*, and *Streptococcus gallolyticus* had weak to moderate positive correlations with Escherichia, while other bacteria showed negative correlations with Escherichia. Of all the bacteria, only *Lactobacillus ruminis* showed no correlation with *Enterococcus saccharolyticus* and *Streptococcus gallolyticus* but had moderate positive correlations with other organisms. Interestingly, SCFAs producing gut microbiota including *Gemmiger formicilis, Blautia schinkii, Blautia faecis, Collinsella aerofaciens, Blautia luti, Blautia wexlera*e, and *Bifidobacterium longum* were all strongly positively correlated. Furthermore, the result of the network analysis corroborated the Spearman's rank correlation, as 93% and 80% of the organisms were negatively correlated with *Enterococcus saccharolyticus* and Escherichia, respectively, with $r > 0.2$. The results indicate metabolic pathways-dependent complex ecological interactions exist among gut microbiota.

Discussions

Utilization of RSM for DES parameter optimization in natural polysaccharide extraction has been well-documented [20]. This optimization study highlights the significant impact of pH, temperature, solid–liquid ratio,

pretreatment time, amplitude, and sonication time on polysaccharide yield within the experimental range. The Mw of our extracted UPS is consistent with those reported by Zuofa et al. [31] (455.6 kDa) but higher than Liu et al. [32] (151 kDa). High Mw polysaccharides are known for enhanced functionality due to their complex structure and interactions [33, 34]. The elevated Mw of our UPS suggests non-degradative ultrasound processing and efficient DES extraction. Monosaccharide composition analysis aligns with previous studies, confirming the presence of galacturonic acid, galactose, glucose, arabinose, and fructose [34, 35]. Monosaccharide components correlate with polysaccharide bio-functionalities [32].

FTIR spectroscopy effectively evaluates functional groups in plant polysaccharides [36]. O–H stretching and unique UPS fingerprint region validates our monosaccharide composition, which is consistent with previous findings [36, 37]. A structure–function relationship of polysaccharides containing one or more of COOH, OH, and COH has also been reported [38, 39]. The peaks indicating carboxylic groups (1729.54 cm^{-1} and 1502.97 cm^{-1}) are traceable to the presence of uronic acids from the galacturonic acid components of the monosaccharides and this resembles date flesh polysaccharides at 1650 cm^{-1} [36]. Interestingly, improved antioxidant properties have been associated with uronic acid components of polysaccharides [38]. The presence of α- and β-conformation pyranose ring regions aligns with prior research [13, 36]. C–H bending variation in our UPS is similar to ginger polysaccharides [40].

Polysaccharide suitability in the food and pharmaceutical industries depends on thermal behavior [38]. Double endothermic peaks in DSC suggest water-retaining ability due to hydrophilic ends, with a single exothermic peak linked to the chemical profile. UPS melting temperature (T_m) and thermal decomposition temperature (T_d) are comparable to pectic polysaccharides at 105 °C and 220 °C [41], indicating UPS's high melting point and thermal stability due to its Mw, monosaccharaide composition and structural bonds [32]. UPS may exhibit stability during heating and industrial processes. In TGA, the initial 12.5% loss is attributed to compound volatilization, while subsequent 37.5% mass losses relate to structural thermal decomposition. Remaining mass at 600 °C becomes ash [20]. Scanning electron microscopy (SEM) reveals a compact morphological structure with high aggregation [42], akin to ultrasonically extracted date flesh polysaccharides (DFP) [36]. High Mw and rigid structure imply UPS's potential as a viscosity enhancer.

UPS particle size exceeds Ayyash et al. [43] and Ali et al. [16] is attributed to source, pretreatment, and extraction conditions. UPS zeta potential is similar to EPS-M41 (−249.63 mV), likely due to hydroxyl and carboxyl group presence. Negatively charged polysaccharides are reported to possess significant bioactivities. Particle size and zeta potential vary among polysaccharides due to differences in Mw, monosaccharide components, and functional groups [44].

Dynamic measurement of viscoelastic properties, including storage (G') and loss (G") moduli, effectively clarifies the predominance of elastic and viscous properties in polysaccharide behavior [45]. We characterized the solid and liquid properties of UPS using a frequency sweep test. The dominance of G' magnitude over G" in both amplitude and frequency sweep tests suggests UPS is more elastic than viscous, aligning with previous studies [45]. These results are consistent with Liao et al. [45] but diverge from Han et al. [46], possibly due to variations in monosaccharide moieties, Mw, glycosidic bonds, and functional groups [47]. Polysaccharides exhibit time-dependent behavior, involving structural deterioration and recovery under strain-shearing time conditions. Our time-dependent test indicates UPS displays elastic properties under low shear and viscous properties under high shear, aligning with previous findings [16], UPS shows promise as a thickening agent in the food and pharmaceutical industries, withstanding rigorous industrial processes. Further exploration of UPS's rheological properties in food systems with other solutes is warranted.

Biomacromolecules like lipids, proteins, and nucleic acids are susceptible to oxidative stress from excess free radicals, leading to inflammation, aging, and tumor growth [5]. Polysaccharides have emerged as natural antioxidants for scavenging free radicals [36]. At 1000 mg/L, UPS exhibits higher DPPH activity (55.0%) compared to 10 mg/mL [13]. Similarly, UPS shows greater ABTS activity than DFP [36]. Oxygen-dependent metabolic pathways generate reactive oxygen species (ROS), pivotal in signal transduction but harmful in excess. SD and SAS activities are comparable to previous study [16]. The presence of functional groups in polysaccharides makes them effective scavengers of hydroxyl radicals [8]. UPS exhibits higher HP and HRS activities at 1 mg/mL than the 25.5% and 26.6% inhibition at 5 mg/mL [36].

Polysaccharide chelation of metallic ions has garnered attention, influenced by hydroxyl group accessibility and cross-bridges with divalent ions [8]. The metal chelation (MC) assay shows UPS's effective binding capacity with ferrozine, surpassing previous reports [48]. The FRAP assay evaluates UPS's potential to donate electrons, with UPS exceeding 1.34 mM [13]. Reduction of Fe^{3+} to Fe^{2+} assesses UPS's reducing power, similar to Shafie and Gan [13]. UPS demonstrates excellent TAC, which is significantly higher than Adebayo-Tayo et al. [49]. In summary, UPS possesses broad-spectrum antioxidant capacity,

potentially serving as a natural antioxidant source. Low IC_{50} values indicate UPS's effectiveness at low concentrations with low system toxicity. Variations in antioxidant capacities result from factors like Mw, monosaccharide components, functional groups, and unmethylated acidic groups [33, 50]. In conclusion, UPS shows significant concentration-dependent in vitro scavenging activities, promising as a functional food ingredient. Further investigation is needed to understand its bioavailability and bio-accessibility in the body.

Sugar-induced type-II diabetes mellitus and postprandial hyperglycemia can be managed through α-amylase and α-glucosidase inhibition [44]. UPS's inhibition of α-amylase and α-glucosidase aligns with Meng et al. [44]. Mechanisms of these enzymes are not fully understood, with factors like glycosidic bonds, functional groups, monosaccharide composition, and uronic acid content influencing enzyme–substrate interactions [44].

Regulating cardiovascular diseases such as hypertension can involve ACE-inhibition, which controls the conversion of angiotensin I to angiotensin II, a potent vasoconstrictor [8]. UPS demonstrated significant ACE-inhibition, comparable to Ayyash et al. [51]. In summary, UPS exhibits notable enzyme inhibition activities related to diabetes and hypertension, suggesting its potential as a raw material for developing functional foods or drugs targeting hypoglycemic and hypotensive effects.

Carcinomas play a central role in cancer development and progression. The antiproliferative properties of UPS align with cytotoxicity assays against human carcinoma cells, with concentrations and IC_{50} values higher than our investigation [43]. While cytotoxicity mechanisms of polysaccharides require further study, potential contributors include immune system stimulation, induced apoptosis, and oncogene expression alterations [52]. In summary, our study highlights UPS's potential as a natural antitumor agent for human colon and breast cancer cells in vitro.

UPS demonstrated significant antibacterial activity against tested pathogens, with lower concentrations compared to previous reports, though variations occurred among bacterial species. Our results indicated higher *E. coli* O157:H7 reduction than *S.* Typhimurium, aligning with Ali et al. [16]. Additionally, UPS showed stronger inhibition of Gram-negative bacteria compared to Gram-positive bacteria, consistent with Yu et al. [52]. Our MIC (500 mg/L) was lower than the reported 6.3 mg/mL [53]. These differences may relate to factors such as molecular weight, zeta potential, monosaccharide content, and functional groups [33]. While antimicrobial mechanisms of polysaccharides remain poorly understood, potential factors include auto-aggregation, hydrophobicity, cell wall disruption, and nutrient blockage [46]. In summary, UPS demonstrates potential as a broad-spectrum antimicrobial agent suitable for applications in the food and pharmaceutical industries.

Functional indicators like WBC, FBC, and WSI are essential in food processing and texture development [22]. UPS exhibited a strong capacity to bind water and oil and water solubility, reflected in WBC, FBC, and WSI values. Our WBC exceeded Jia et al. [22] but aligned with Ali et al. [16]. Similarly, our FBC was comparable to Jia et al. [22] but higher than Noorbakhsh and Khorasgani [37]. High WBC reduces syneresis, modifies viscosity, and impacts texture, while FBC relates to flavor preservation [16]. Our WSI matched Ali et al. [16]. Differences in WBC may stem from variations in Mw, conformation, functional groups, and glycosidic bonds, while FBC can be influenced by porosity, chemical components, and hypolipidemic activity, and WSI can vary due to factors like particle size and hydrogen bonding [16, 37].

Plant polysaccharides are recognized as natural prebiotics due to their resistance to upper gut digestion and metabolism by colonic microbiota [33]. Our findings, consistent with Wu et al. [10], reveal the prebiotic potential of UPS through bacterial growth kinetics. This effect is characterized by selective stimulation of probiotic strains' growth and survival, though outcomes vary with carbon sources and growth kinetics. The reduced lag phase for UPS suggests it serves as a readily metabolizable energy source for probiotics, aligning with Noorbakhsh and Khorasgani [37]. Dynamic changes in gas production and pH may result from microbial degradation and utilization of polysaccharides, producing SCFAs [37]. Total and reducing sugar results reflect microbial utilization of polysaccharides to produce reducing ends, used by other specific microbes [46]. Microbial degradation of plant polysaccharides yields prebiotic metabolites, including acetic, propionic, and butyric acids, which modulate gut microbial ecology [10].

Our SCFA analysis results align with the observed low pH of UPS fermentation, attributed to the synthesis of acidic SCFAs. Generally, UPS demonstrated SCFA production similar to GOS-P and significantly higher than the control group, suggesting UPS as a potential energy source for human gut microbiota. SCFA production order from fermented UPS was acetic, propionic, and butyric acid, consistent with prior study [54]. Acetic acid serves as an energy source in peripheral tissues, enhancing glucose tolerance and insulin production [10]. Propionic acid influences cholesterol modulation, insulin metabolism, glucose uptake, and lipogenesis, while butyric acid is linked to preventing intestinal damage, obesity, and diabetes [54].

In our study, the UPS group exhibited the highest Shannon index mean and the lowest Simpson index

mean. This suggests lower microbial diversity but higher evenness in the UPS-treated fermentation broth, in line with previous findings [46, 54]. The separation of UPS and GOS-P from the control group in NMDS and PCoA plots indicates a positive microbial association between UPS and GOS-P due to treatment and fecal microbiota metabolic activities. Analysis of OTUs, alpha and beta diversities revealed significant differences in gut microbiota diversity, distribution, microbial community characterization, and species complexities.

The relative abundance of Firmicutes, Bacteroides, and Proteobacteria phyla constituted over 95% of the total microbiota, slightly different from studies reporting more than 90% of gut microbiota consisting mainly of Firmicutes and Bacteroides [54]. Notably, UPS exhibited a low Firmicutes/Bacteroidetes (F/B) ratio, a key anti-obesity biomarker [55]. UPS and GOS-P had significantly higher abundance of the Clostridiales and Bifidobacteriales orders, favoring SCFAs synthesis [54]. Compared to the control group, UPS and GOS-P showed higher abundance of Actinobacteria, important for anticholesterol activities [55]. Similarly, at the genus level, UPS and GOS-P displayed higher relative abundance of Bifidobacterium and Blautia, essential SCFA producers and polysaccharide hydrolyzers, contributing to reduced hypercholesterolemia [55].

In summary, our microbial composition and abundance during fermentation indicate changes in microflora abundance across different taxonomic ranks. This suggests that including UPS in the fermentation broth acts as a prebiotic, promoting the proliferation and diversification of gut microbiota. The observed differences in KEGG, COG, and MetaCyc prediction analysis imply that including UPS in the fermentation process exerts prebiotic potential on the gut microbiome, influencing the diversity of metabolic pathways and metabolites required for the survival and growth of beneficial bacteria contributing to host health [55]. However, while UPS shows promise for developing functional foods targeting specific gut bacteria, metabolites, and metabolic pathways, further real-time experimental confirmation is needed to validate computer simulation results. The strong negative correlation of SCFA producers with opportunistic pathogens may be attributed to the treatment, enhancing the survival and proliferation of beneficial microbes and contributing to gut homeostasis [54].

Conclusion

Physicochemical and structural analyses revealed that UPS is a high molecular weight (Mw) heteropolysaccharide with diverse sugar moieties. Notably, at a concentration of 1000 mg/L, UPS demonstrated potent radical scavenging activities, inhibited both Gram-positive and Gram-negative pathogens, reduced the activity of diabetic and hypertension indicator enzymes, and significantly impeded the proliferation of colon and breast cancer cell lines. UPS exhibited remarkable prebiotic, bioactive, and functional properties, which were notably influenced by its structural features and monosaccharide composition. Additionally, UPS displayed promising results as a carbon source, promoting the growth and survival of probiotics. The fermentation of UPS by colonic microbiota in human fecal matter was evident through the observed reduction in pH and increased gas production. This fermentation led to the synthesis of short-chain fatty acids (SCFAs), which played a crucial role in homeostasis and modulation of microbial composition, growth, diversities, abundances, and metabolite production. The health-promoting results obtained in this study are attributed to the unique chemical structure and functional groups of UPS. Therefore, UPS can be utilized to formulate food and drugs for specific functions. Overall, our study provided a simpler and more environmentally friendly method for extracting date pomace polysaccharides with excellent bioactivities and fecal fermentation characteristics. These findings suggest potential applications as functional food ingredients for gut health. However, further in vivo investigations of UPS are necessary to confirm all the bio-functionalities identified in this study.

Abbreviations

GCC	Gulf Cooperation Council
MENA	Middle East and North Africa
PS	Polysaccharide
DES	Deep eutectic solvents
HBD	Hydrogen bond donors
SCFA	Short-chain fatty acids
DP	Date pomace polysaccharide
ChCl:CA	Choline chloride:citric acid
UPS	Ultrasound extracted polysaccharide
CCD	Central composite design
TCA	Trichloroacetic acid
GPC	Gel permeation chromatography
TFA	Trifluoroacetic acid
PMP	1-Phenyl-3-methyl-5-pyrazolone
FTIR	Fourier transform infrared spectroscopy
PDA	Photodiode array detector
DSC	Differential scanning calorimetry
TGA	Thermo-gravimetric analysis
SEM	Scanning electron microscope
WSI	Water solubility index
WHC	Water holding capacity
OHC	Oil holding capacity
Tg	Glass transition temperature
Tm	Melting point temperature
Td	Degradation temperature
DPPH	1-Diphenyl-2-picrylhydrazyl
ABTS	2,2′-Azino-bis(3-ethylbenzene-thiazoline-6-sulphonic acid
SD	Superoxide dismutase
SAS	Superoxide anion scavenging
TAC	Total antioxidant capacity
FRAP	Ferric reducing antioxidant power
RP	Reducing power

ACE	Angiotensin-converting enzyme
FLASH	Fast length adjustment of short
RS	Reducing sugar
TS	Total sugar
GOS	Galacto-oligosaccharide
NMDS	Non-metric multidimensional scaling
KEGG	Kyoto Encyclopedia of Genes and Genomes
COG	Clusters of orthologous groups
PICRUSt	Phylogenetic Investigation of Communities by Reconstruction of Unobserved States

Supplementary Information

The online version contains supplementary material available at https://doi.org/10.1186/s40538-024-00601-0.

Supplementary material 1: Table S1. CCD with experimental results for DES pretreatment parameters on DP Table S2. ANOVA for regression model effects of DES pretreatment parameters on DP yield Table S3. CCD with experimental results for UAE optimization of DP pretreated with DES. Table S4. Combined ANOVA for regression model effects of UAE parameters on UPS yield and Estimate Figure S1. The Ultrasound polysaccharide (UPS) response surface plot showing the combined effect of DES and UAE conditions on yield of UPS; combined effects of hot water bath extraction time and DES pH (A), DES solid–liquid ratio and pH (B), hot water bath extraction time and DES solid–liquid ratio (C), hot water bath extraction time and temperature (D), hot water bath extraction temperature and DES solid–liquid ratio (E), hot water bath extraction temperature and DES pH (F), and ultrasound time and amplitude (G).Figure S2. (A) Particle size analysis and (B) zeta potential at frequency 8.47 Hz of UPS Figure S3. Quantity of total and reducing sugar of UPS before and after *in vitro* digestion. Bars are means ± standard deviations (error bars). a-b Means with different lowercase letters at the same parameter differed significantly ($P < 0.05$). Figure S4. The Growth Curve of Probiotic Strains *Lactobacillus acidophilus* (A), *Lactobacillus delbrueckii subsp. delbrueckii* (B), *Lacticaseibacillus rhamnosus* (C), *Lacticaseibacillus paracasei subsp. paracasei* (D), *Lactobacillus gasseri* (E), and *Bifidobacterium breve* (F), with UPS (blue line), blank (no sugar, green line), GOS-P (red line), and Glucose (black line). Figure S5. Alpha diversity rarefaction curves of different Indices during *in vitro* fecal fermentation. Ace (A), Chao (B), Observed species (C), Simpson (D), Shannon (E), and Coverage (F) rarefaction curves of the Sample Groups.Where A (red lines), B (blue lines), and D (green lines) represent the sample groups (A) Blank (negative control), (B) GOS-P (positive control) , and (D) UPS. Figure S6. (A) OTU ANOSIM analysis between and within groups, stacked column plot of microbial (B) phylum (C) genus relative abundance, (D) heatmap analysis of relative abundance of top 50 species, (E) network and phylum heatmap of *in vitro* fecal fermentation, and (F) phylum heatmap, where horizontal clusters represent the similarity of species among samples, and relative abundance values are log-transformed. Legends A, B, and D represent sample groups (A) Blank (negative control), (B) GOS-P (positive control), and (D) UPS.

Acknowledgements
We are also grateful to Ms. Shamma Aljinaibi, Ms. Jawaher Alsada, Ms. Reem Saeed Ahmed Saleh for their technical support.

Author contributions
G. Bamigbade: writing—original draft, investigation, visualization, formal analysis; A. Subhash and M. Tarique: methodology, formal analysis; B. al-Ramadi and B. Abu-Jdayil: writing—review & editing; A. Kamal-Eldin and L. Nyström: conceptualization, writing—review & editing; M. Ayyash: conceptualization, writing—review & editing, supervision, project administration, funding acquisition.

Funding
The authors thank the United Arab Emirates University and Zayed Center for Health Sciences (UAEU) for funding this project (grant numbers #12R105 and #12F054).

Availability of data and materials
The datasets used and/or analyzed during the current study are available from the corresponding author on reasonable request.

Declarations

Ethics approval and consent to participate
Not applicable.

Consent for publication
Not applicable.

Competing interests
The authors declare that they have no competing interests.

Author details
[1]Department of Food Science, College of Agriculture and Veterinary Medicine, United Arab Emirates University (UAEU), Al-Ain, UAE. [2]Department of Medical Microbiology and Immunology, College of Medicine and Health Sciences, United Arab Emirates University (UAEU), Al Ain, UAE. [3]Chemical and Petroleum Engineering Department, College of Engineering, United Arab Emirates University (UAEU), PO Box 15551, Al Ain, UAE. [4]Department of Health Science and Technology, Institute of Food, Nutrition and Health, ETH Zurich, 8092 Zurich, Switzerland. [5]Zayed Center for Health Sciences, United Arab Emirates University (UAEU), Al Ain, UAE.

Received: 3 April 2024 Accepted: 24 May 2024
Published online: 04 June 2024

References

1. Subhash AJ, Bamigbade GB, Ayyash M. Current insights into date by-product valorization for sustainable food industries and technology. Sustain Food Technol. 2024. https://doi.org/10.1039/d3fb00224a.
2. Mohamed GR, Mahmoud RK, Shaban M, Fahim IS, Abd El-Salam HM, Mahmoud HM. Towards a circular economy: valorization of banana peels by developing bio-composites thermal insulators. Sci Rep. 2023;13(1):12756. https://doi.org/10.1038/s41598-023-37994-1.
3. Hu T, Lin Q, Guo T, Yang T, Zhou W, Deng X, et al. Polysaccharide isolated from Phellinus linteus mycelia exerts anti-inflammatory effects via MAPK and PPAR signaling pathways. Carbohydr Polym. 2018;200:487–97. https://doi.org/10.1016/j.carbpol.2018.08.021.
4. Zhan K, Ji X, Luo L. Recent progress in research on Momordica charantia polysaccharides: extraction, purification, structural characteristics and bioactivities. Chem Biol Technol Agric. 2023;10(1):58. https://doi.org/10.1186/s40538-023-00433-4.
5. Saadat RY, Yari Khosroushahi A, Pourghassem GB. A comprehensive review of anticancer, immunomodulatory and health beneficial effects of the lactic acid bacteria exopolysaccharides. Carbohydr Polym. 2019;217:79–89. https://doi.org/10.1016/j.carbpol.2019.04.025.
6. Ji X, Peng Q, Yuan Y, Shen J, Xie X, Wang M. Isolation, structures and bioactivities of the polysaccharides from jujube fruit (*Ziziphus jujuba Mill.*): a review. Food Chem. 2017;227:349–57. https://doi.org/10.1016/j.foodchem.2017.01.074.
7. Koropatkin NM, Cameron EA, Martens EC. How glycan metabolism shapes the human gut microbiota. Nat Rev Microbiol. 2012;10(5):323–35. https://doi.org/10.1038/nrmicro2746.
8. Wang D, Zhang BB, Qu XX, Gao F, Yuan MY. Microwave-assisted extraction of polysaccharides from Yupingfeng powder and their antioxidant activity. Pharmacogn Mag. 2015;11(43):546–54. https://doi.org/10.4103/0973-1296.160468.
9. Zdanowicz M, Wilpiszewska K, Spychaj T. Deep eutectic solvents for polysaccharides processing A review. Carbohydr Polym. 2018;200:361–80. https://doi.org/10.1016/j.carbpol.2018.07.078.
10. Wu DT, Fu MX, Guo H, Hu YC, Zheng XQ, Gan RY, Zou L. Microwave-assisted deep eutectic solvent extraction, structural characteristics, and biological functions of polysaccharides from sweet tea (*Lithocarpus*

litseifolius) leaves. Antioxidants. 2022;11(8):1578. https://doi.org/10.3390/antiox11081578.
11. Cui R, Zhu F. Ultrasound modified polysaccharides: a review of structure, physicochemical properties, biological activities and food applications. Trends Food Sci Technol. 2021;107:491–508. https://doi.org/10.1016/j.tifs.2020.11.018.
12. Hu J-L, Nie S-P, Li C, Wang S, Xie M-Y. Ultrasonic irradiation induces degradation and improves prebiotic properties of polysaccharide from seeds of *Plantago asiatica* L. during in vitro fermentation by human fecal microbiota. Food Hydrocoll. 2018;76:60–6. https://doi.org/10.1016/j.foodhyd.2017.06.009.
13. Shafie MH, Gan C-Y. Could choline chloride-citric acid monohydrate molar ratio in deep eutectic solvent affect structural, functional and antioxidant properties of pectin? Int J Biol Macromol. 2020;149:835–43. https://doi.org/10.1016/j.ijbiomac.2020.02.013.
14. Yang J, Zamani S, Liang L, Chen L. Extraction methods significantly impact pea protein composition, structure and gelling properties. Food Hydrocoll. 2021;117: 106678. https://doi.org/10.1016/j.foodhyd.2021.106678.
15. Cuesta G, Suarez N, Bessio MI, Ferreira F, Massaldi H. Quantitative determination of pneumococcal capsular polysaccharide serotype 14 using a modification of phenol-sulfuric acid method. J Microbiol Methods. 2003;52(1):69–73. https://doi.org/10.1016/s0167-7012(02)00151-3.
16. Ali AH, Bamigbade G, Tarique M, Esposito G, Obaid R, Abu-Jdayil B, Ayyash M. Physicochemical, rheological, and bioactive properties of exopolysaccharide produced by a potential probiotic Enterococcus faecalis 84B. Int J Biol Macromol. 2023;240:124425. https://doi.org/10.1016/j.ijbiomac.2023.124425.
17. Bamigbade GB, Subhash AJ, Al-Ramadi B, Kamal-Eldin A, Gan R-Y, Liu SQ, Ayyash M. Gut microbiota modulation, prebiotic and bioactive characteristics of date pomace polysaccharides extracted by microwave-assisted deep eutectic solvent. Int J Biol Macromol. 2024;262:130167. https://doi.org/10.1016/j.ijbiomac.2024.130167.
18. Qiao Q, Song X, Zhang C, Jiang C, Jiang R. Structure and immunostimulating activity of polysaccharides derived from the roots and leaves of dandelion. Chem Biol Technol Agric. 2024;11(1):51. https://doi.org/10.1186/s40538-024-00568-y.
19. Sasikumar K, Kozhummal Vaikkath D, Devendra L, Nampoothiri KM. An exopolysaccharide (EPS) from a Lactobacillus plantarum BR2 with potential benefits for making functional foods. Bioresour Technol. 2017;241:1152–6. https://doi.org/10.1016/j.biortech.2017.05.075.
20. Fatahi F, Tabaraki R. Deep eutectic solvent mediated extraction of polysaccharides and antioxidants from Persian manna (Taranjabin): Comparison of different extraction methods and optimization by response surface methodology. Microchem J. 2023;194:109336. https://doi.org/10.1016/j.microc.2023.109336.
21. Rütering M, Schmid J, Gansbiller M, Braun A, Kleinen J, Schilling M, Sieber V. Rheological characterization of the exopolysaccharide Paenan in surfactant systems. Carbohydr Polym. 2018;181:719–26. https://doi.org/10.1016/j.carbpol.2017.11.086.
22. Jia K, Tao X, Liu Z, Zhan H, He W, Zhang Z, et al. Characterization of novel exopolysaccharide of Enterococcus faecium WEFA23 from infant and demonstration of its in vitro biological properties. Int J Biol Macromol. 2019;128:710–7. https://doi.org/10.1016/j.ijbiomac.2018.12.245.
23. Tarique M, Ali AH, Kizhakkayil J, Liu S-Q, Oz F, Dertli E, et al. Exopolysaccharides from Enterococcus faecium and Streptococcus thermophilus: bioactivities, gut microbiome effects, and fermented milk rheology. Food Chem:X. 2024;21:101073. https://doi.org/10.1016/j.fochx.2023.101073.
24. Subhash AJ, Babatunde Bamigbade G, Al-Ramadi B, Kamal-Eldin A, Gan R-Y, Senaka Ranadheera C, Ayyash M. Characterizing date seed polysaccharides: a comprehensive study on extraction, biological activities, prebiotic potential, gut microbiota modulation, and rheology using microwave-assisted deep eutectic solvent. Food Chem. 2024;444:138618. https://doi.org/10.1016/j.foodchem.2024.138618.
25. Brodkorb A, Egger L, Alminger M, Alvito P, Assunção R, Ballance S, et al. INFOGEST static in vitro simulation of gastrointestinal food digestion. Nat Protoc. 2019;14(4):991–1014. https://doi.org/10.1038/s41596-018-0119-1.
26. Yılmaz T, Şimşek Ö. Potential health benefits of ropy exopolysaccharides produced by Lactobacillus plantarum. Molecules. 2020;25(14):3293. https://doi.org/10.3390/molecules25143293.
27. Dobrowolska-Iwanek J, Lauterbach R, Huras H, Paśko P, Prochownik E, Woźniakiewicz M, et al. HPLC-DAD method for the quantitative determination of short-chain fatty acids in meconium samples. Microchem J. 2020;155:104671. https://doi.org/10.1016/j.microc.2020.104671.
28. Wu J, Li C, Bai L, Wu J, Bo R, Ye M, et al. Structural differences of polysaccharides from Astragalus before and after honey processing and their effects on colitis mice. Int J Biol Macromol. 2021;182:815–24. https://doi.org/10.1016/j.ijbiomac.2021.04.055.
29. Jiao L, Li J, Liu F, Wang J, Jiang P, Li B, et al. Characterisation, chain conformation and antifatigue effect of steamed ginseng polysaccharides with different molecular weight. Front Pharmacol. 2021. https://doi.org/10.3389/fphar.2021.712836.
30. Subhash AJ, Bamigbade GB, Tarique M, Al-Ramadi B, Abu-Jdayil B, Kamal-Eldin A, et al. Bioactive properties and gut microbiota modulation by date seed polysaccharides extracted using ultrasound-assisted deep eutectic solvent. Food Chem:X. 2024;22:101354. https://doi.org/10.1016/j.fochx.2024.101354.
31. Zuofa Z, Tingting S, Guoying L, Jie L, Qunli J. Structural properties and immunomodulatory activity of an α-glucan purified from the fruiting body of Stropharia rugosoannulata. Chem Biol Technol Agric. 2023;10(1):100. https://doi.org/10.1186/s40538-023-00475-8.
32. Liu M, Wang Y, Wang R, Du Q, Wang L. Structural characterization, physicochemical property, and antioxidant activity of polysaccharide components from Eucommia ulmoides leaves. Chem Biol Technol Agric. 2023;10(1):122. https://doi.org/10.1186/s40538-023-00495-4.
33. Tiwari S, Kavitake D, Devi PB, Halady SP. Bacterial exopolysaccharides for improvement of technological, functional and rheological properties of yoghurt. Int J Biol Macromol. 2021;183:1585–95. https://doi.org/10.1016/j.ijbiomac.2021.05.140.
34. Zhou L, Luo S, Li J, Zhou Y, Wang X, Kong Q, et al. Optimization of the extraction of polysaccharides from the shells of Camellia oleifera and evaluation on the antioxidant potential in vitro and in vivo. J Functional Foods. 2021;86:104678. https://doi.org/10.1016/j.jff.2021.104678.
35. Zhou S, Huang G. Extraction, structure characterization and biological activity of polysaccharide from coconut peel. Chem Biol Technol Agric. 2023;10(1):15. https://doi.org/10.1186/s40538-023-00391-x.
36. Dhahri M, Sioud S, Alsuhaymi S, Almulhim F, Haneef A, Saoudi A, et al. Extraction, characterization, and antioxidant activity of polysaccharides from Ajwa Seed and Flesh. Separations. 2023;10(2):103. https://doi.org/10.3390/separations10020103.
37. Noorbakhsh H, Khorasgani MR. Functional and chemical properties of Phoenix dactylifera l. Polysaccharides and the effect of date flesh and seed intervention on some blood biomarkers: A contrastive analysis. Food Chem:X. 2023;19:100834. https://doi.org/10.1016/j.fochx.2023.100834.
38. Chai Z, Huang W, Zhao X, Wu H, Zeng X, Li C. Preparation, characterization, antioxidant activity and protective effect against cellular oxidative stress of polysaccharide from Cynanchum auriculatum Royle ex Wight. Int J Biol Macromol. 2018;119:1068–76. https://doi.org/10.1016/j.ijbiomac.2018.08.024.
39. Wang J, Hu S, Nie S, Yu Q, Xie M. Reviews on Mechanisms of In vitro antioxidant activity of polysaccharides. Oxid Med Cell Longev. 2016;2016:5692852. https://doi.org/10.1155/2016/5692852.
40. Zhou S, Wang X, Jiang W, Tan J, Chen G. Preparation, structural characterization and in vitro activity of ginger polysaccharide. Chem Biol Technol Agric. 2023;10(1):126. https://doi.org/10.1186/s40538-023-00498-1.
41. Wang X, Lü X. Characterization of pectic polysaccharides extracted from apple pomace by hot-compressed water. Carbohydr Polym. 2014;102:174–84. https://doi.org/10.1016/j.carbpol.2013.11.012.
42. Ji X, Cheng Y, Tian J, Zhang S, Jing Y, Shi M. Structural characterization of polysaccharide from jujube (*Ziziphus jujuba Mill.*) fruit. Chem Biol Technol Agric. 2021;8(1):54. https://doi.org/10.1186/s40538-021-00255-2.
43. Ayyash M, Abu-Jdayil B, Olaimat A, Esposito G, Itsaranuwat P, Osaili T, et al. Physicochemical, bioactive and rheological properties of an exopolysaccharide produced by a probiotic Pediococcus pentosaceus M41. Carbohydr Polym. 2020;229:115462. https://doi.org/10.1016/j.carbpol.2019.115462.
44. Meng M, Guo M, Wang P, Han R, Zhou J, Wang C. Chemopreventive effect of the polysaccharides from Grifola frondosa in colitis-associated colorectal cancer by modulating the Wnt/β-catenin/GSK-3β signaling pathway

in C57BL/6 mice. J Functional Foods. 2019;63:103578. https://doi.org/10.1016/j.jff.2019.103578.
45. Liao B-Y, Li L, Tanase C, Thakur K, Zhu D-Y, Zhang J-G, Wei Z-J. The rheological behavior of polysaccharides from Mulberry leaves (*Morus alba L.*). Agronomy. 2020;10(9):1267. https://doi.org/10.3390/agronomy10091267.
46. Han X, Zhou Q, Gao Z, Lin X, Zhou K, Cheng X, et al. In vitro digestion and fecal fermentation behaviors of polysaccharides from Ziziphus Jujuba cv. Pozao and its interaction with human gut microbiota. Food Res Int. 2022;162:112022. https://doi.org/10.1016/j.foodres.2022.112022.
47. Li X, Chen J, Yin Y, Xiao S, Zhang R, Yang Y, et al. Chemical structure elucidation and functional activities comparison of two polysaccharides purified from Citrus reticulata Blanco peels. Chem Biol Technol Agric. 2024;11(1):37. https://doi.org/10.1186/s40538-024-00556-2.
48. Nikitina E, Petrova T, Sungatullina A, Bondar O, Kharina M, Mikshina P, et al. The profile of exopolysaccharides produced by various lactobacillus species from silage during not-fat milk fermentation. Fermentation. 2023;9(2):197. https://doi.org/10.3390/fermentation9020197.
49. Adebayo-Tayo B, Ishola R, Oyewunmi T. Characterization, antioxidant and immunomodulatory potential on exopolysaccharide produced by wild type and mutant Weissella confusa strains. Biotechnol Rep. 2018;19:e00271. https://doi.org/10.1016/j.btre.2018.e00271.
50. Ji X, Guo J, Ding D, Gao J, Hao L, Guo X, Liu Y. Structural characterization and antioxidant activity of a novel high-molecular-weight polysaccharide from *Ziziphus Jujuba* cv Muzao. J Food Measurement Charact. 2022;16(3):2191–200. https://doi.org/10.1007/s11694-022-01288-3.
51. Ayyash M, Al-Nuaimi AK, Al-Mahadin S, Liu S-Q. In vitro investigation of anticancer and ACE-inhibiting activity, α-amylase and α-glucosidase inhibition, and antioxidant activity of camel milk fermented with camel milk probiotic: a comparative study with fermented bovine milk. Food Chem. 2018;239:588–97. https://doi.org/10.1016/j.foodchem.2017.06.149.
52. Yu Z, Li Y, Li Y, Zhang J, Li M, Ji L, et al. Bufalin stimulates antitumor immune response by driving tumor-infiltrating macrophage toward M1 phenotype in hepatocellular carcinoma. J Immunother Cancer. 2022. https://doi.org/10.1136/jitc-2021-004297.
53. Khlusov I, Avdeeva E, Shupletsova V, Khaziakhmatova O, Litvinova L, Porokhova E, et al. Comparative in vitro evaluation of antibacterial and osteogenic activity of polysaccharide and flavonoid fractions isolated from the leaves of saussurea controversa. Molecules. 2019;24(20):3680. https://doi.org/10.3390/molecules24203680.
54. Yi C, Xu L, Luo C, He H, Ai X, Zhu H. In vitro digestion, fecal fermentation, and gut bacteria regulation of brown rice gel prepared from rice slurry backfilled with rice bran. Food Hydrocoll. 2022;133:107986. https://doi.org/10.1016/j.foodhyd.2022.107986.
55. Chen L, Pu Y, Xu Y, He X, Cao J, Ma Y, Jiang W. Anti-diabetic and anti-obesity: efficacy evaluation and exploitation of polyphenols in fruits and vegetables. Food Res Int. 2022;157:111202. https://doi.org/10.1016/j.foodres.2022.111202.

Publisher's Note